Article

pubs.acs.org/Biomac

Dehydrodipeptide Hydrogelators Containing Naproxen *N*-Capped Tryptophan: Self-Assembly, Hydrogel Characterization, and Evaluation as Potential Drug Nanocarriers

Helena Vilaça,[†] Ana C. L. Hortelão,[‡] Elisabete M. S. Castanheira,*[,‡] Maria-João R. P. Queiroz,[†] Loic Hilliou,[§] Ian W. Hamley,[⊥] José A. Martins,*[,†] and Paula M. T. Ferreira*[,†]

[†]Centre of Chemistry and [‡]Centre of Physics, University of Minho, Campus de Gualtar, 4710-057 Braga, Portugal

[§]Institute for Polymers and Composites/I3N, Department of Polymer Engineering, University of Minho, Campus de Azurém, 4800-058 Guimarães, Portugal

[⊥]Department of Chemistry, University of Reading, Whiteknights, P.O. Box 224, Reading RG6 6AD, U.K.

Supporting Information

ABSTRACT: In this work, we introduce dipeptides containing tryptophan *N*-capped with the nonsteroidal anti-inflammatory drug naproxen and *C*-terminal dehydroamino acids, dehydrophenylalanine (ΔPhe), dehydroaminobutyric acid (ΔAbu), and dehydroalanine (ΔAla) as efficacious protease resistant hydrogelators. Optimized conditions for gel formation are reported. Transmission electron microscopy experiments revealed that the hydrogels consist of networks of micro/nanosized fibers formed by peptide self-assembly. Fluorescence and circular dichroism spectroscopy indicate that the self-assembly process is driven by stacking interactions of the aromatic groups. The naphthalene groups of the naproxen moieties are highly organized in the fibers through chiral stacking. Rheological experiments demonstrated that the most hydrophobic peptide (containing *C*-terminal ΔPhe) formed more elastic gels at lower critical gelation concentrations. This gel revealed irreversible breakup, while the *C*-terminal ΔAbu and ΔAla gels, although less elastic, exhibited structural recovery and partial healing of the elastic properties. A potential antitumor thieno[3,2-*b*]pyridine derivative was incorporated (noncovalently) into the gel formed by the hydrogelator containing *C*-terminal ΔPhe residue. Fluorescence and Förster resonance energy transfer measurements indicate that the drug is located in a hydrophobic environment, near/associated with the peptide fibers, establishing this type of hydrogel as a good drug-nanocarrier candidate.

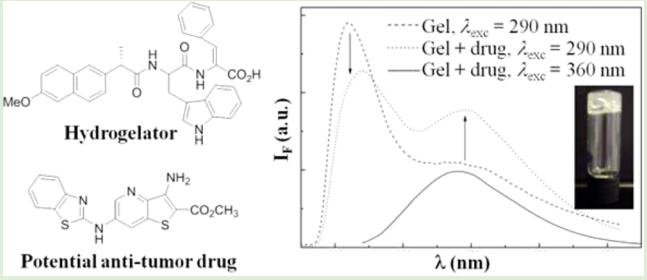

INTRODUCTION

The nanotechnology paradigm is revolutionizing science and technology. The bottom-up approach to functional nanoobjects relies on the hierarchical self-assembly of low molecular weight building blocks. Amino acids and peptides are nature's preferred building blocks. Low molecular weight supramolecular hydrogelators are compounds that, upon a trigger, form a three-dimensional network of entangled fibers that traps water, thus giving a gel. Several methods have been used to trigger gelation: pH,[1] temperature,[2,3] enzymatic catalysis,[4] metal ions,[5,6] or sonication.[7,8] High water content, biocompatibility, and similarity to the extracellular matrix make supramolecular gelators attractive for a wide range of biomedical applications, for example, wound healing,[9,10] drug delivery,[11] biosensing,[12,13] and cell culture.[14,15] Hydrogels made of small peptides, especially di- and tripeptides, are particularly attractive owing to easy synthesis, chemical variability, and potential for introduction of biological functionality. The gelation of this type of peptide is usually driven by the cooperative effect of an ensemble of weak intermolecular interactions: hydrogen bonding, hydrophobic and aromatic $\pi-\pi$ interactions. Susceptibility to enzymatic hydrolysis is the main limitation to widespread use of peptide-based pharmaceuticals, in general, and peptide hydrogels in particular. Replacing natural amino acids by nonproteinogenic analogues, D-amino acids,[1a,12,16,17] β-amino acids,[18] or dehydroamino acids[3,19,20] is a well-established strategy to endow peptides and proteins with proteolytic stability. Despite the variety of dehydroamino acids found in natural sources, dehydrophenylalanine (ΔPhe) in the cyclic tetrapeptide tentoxin, dehydrovaline (ΔVal) in penicillin and cephalosporin, and dehydrotryptophan (ΔTrp) in neochinulins,[21] only ΔPhe has been incorporated recently into peptide hydrogelators.[3,20] Our group has recently reported the incorporation of ΔPhe and dehydroaminobutyric acid (ΔAbu) in naproxen-dipeptide hydrogelators exhibiting resistance to chymotrypsin proteolysis.[22]

Tryptophan (Trp) is a bulky aromatic amino acid with an indole side chain, capable of both hydrogen-bonding and

Received: July 29, 2015
Revised: September 23, 2015
Published: October 7, 2015

DOI: 10.1021/acs.biomac.5b01006
Biomacromolecules 2015, 16, 3562−3573

aromatic interactions. Trp residues in proteins are the most efficient UV light absorbers, responsible for the fluorescence properties of proteins. Changes of absorption or fluorescence emission of proteins can be used for monitoring processes that result in changes of polarity of the local environment of the Trp residues: denaturation of proteins and ligand binding. As far as we know, there are only a few literature reports on indole-containing peptide gelators, a pyrene-Trp[23] and an indole-diphenylalanine hydrogel.[24] Peptide hydrogelators are usually *N*-capped with aromatic moieties such as Fmoc[12,15,25,26] or naphthalene derivatives.[27] Besides tuning hydrogelator solubility and hydrophobicity and increasing the potential for intermolecular aromatic interactions, the capping group itself can be an active drug. The pharmacological properties of the drug can be retained by the hydrogelator (and the hydrogel) or the drug can be released through chemical or enzymatic stimuli. Naproxen (Npx) is a nonsteroidal anti-inflammatory drug (NSAID) belonging to the aryl propionic acid family of nonselective inhibitors of the Cyclooxygenase (COX) enzyme family. Hydrogelators *N*-capped with naproxen not only retain the inhibitory properties of naproxen, but also exhibit enhanced selectivity toward COX-2.[11c,28,29] Hydrogels bearing naproxen are potential candidates for topical treatment of acute or chronic pain or inflammation.[28]

In this work, dipeptides containing Trp *N*-conjugated with naproxen and *C*-terminal dehydroamino acids, ΔPhe, ΔAbu, and dehydroalanine (ΔAla), were synthesized and evaluated as novel hydrogelators. Temperature changes and different methods to drop the pH were tested for triggering gelation. The naproxen moiety was used as an intrinsic fluorescence reporter to determine the pH and concentration of gelation.[22] Circular dichroism (CD), transmission electron microscopy (TEM), and rheology were used to get insight into the self-assembly process and the nano/microstructure of the gel. The ability of this type of hydrogel to act as drug nanocarrier was investigated using a potential antitumor thieno[3,2-*b*]pyridine derivative.[30] Allying proteolytic stability to potential anti-inflammatory properties and drug delivery makes this type of hydrogel promising nanopharmaceuticals.

MATERIALS AND METHODS

General. Melting points (mp, °C) were measured in a Gallenkamp apparatus and are uncorrected. ^{1}H and ^{13}C NMR spectra were recorded on a Bruker Avance III at 400 and 100.6 MHz, respectively, and in a Varian Unity Plus 300 at 300 and 75.4 MHz, respectively. $^{1}H-^{1}H$ spin−spin decoupling and DEPT θ 45° were used. HMQC and HMBC were used to attribute some signals. Chemical shifts (δ) are reported in parts per million (ppm) downfield from tetramethylsilane (TMS), and coupling constants (J) are reported in hertz (Hz). High-resolution mass spectrometry (HRMS) data were provided by the MS service of the University of Vigo, Spain. Elemental analysis was performed on a LECO CHNS 932 elemental analyzer. Column chromatography was performed on Macherey-Nagel silica gel 230−400 mesh. Petroleum ether refers to the boiling range of 40−60 °C. Reactions were monitored by thin-layer chromatography (TLC), using precoated TLC-sheets Alugram Xtra SIL G/UV254, with revelation under UV light (254 nm). Acetonitrile (ACN) was dried over silica and calcium hydride (CaH_2) and then distilled and stored over molecular sieves.

Self-Assembly. All solutions were made up with ultrafiltered (18 MΩ) water from a Barnstead Nanopure system. Phosphate buffer was prepared from sodium dihydrogen phosphate monohydrate ($NaH_2PO_4.H_2O$, Fluka BioChemika) and sodium phosphate dibasic dodecahydrate ($Na_2HPO_4.12H_2O$, Fluka) with a final concentration of 0.1 M and pH 6.00, 7.19, or 8.06 (Mettler Toledo FiveEasy pH Meter). D-Glucono-δ-lactone (GdL, Sigma), aqueous NaOH 1 M, and HCl 0.1 M were used for the gelation experiments.

Self-Assembly in Buffer. Dehydrodipeptides were weighted into sample vials. Buffer was added, and the mixture was sonicated for a few minutes. For peptides that did not dissolve, the mixture was heated to 80 °C in a sonicated bath, left to cool at room temperature, and observed for 1 day.

Self-Assembly with GdL. Compounds were weighed into a sample vial. Water and aqueous NaOH 1 M were added. The mixture was heated to 80 °C in a sonicated bath, left to cool for a few minutes, added to gluconic acid (GdL), and stirred at 1000 rpm for 10 s. The solution was left standing at room temperature overnight, and the pH was measured.

Self-Assembly with HCl. Compounds were weighted into a sample vial. Water and aqueous NaOH 1 M were added. The mixture was heated to 80 °C in a sonicated bath and left to cool for a few minutes. HCl 0.1 M was added until the solution turning slightly turbid. The solution was left standing at room temperature overnight, and the pH was measured.

Circular Dichroism. CD spectra were recorded at 20 °C on a Chirascan spectropolarimeter (Applied Photophysics, UK). Peptide hydrogels were loaded into 0.1 mm quartz cells. Spectra display absorbance <2 at any measured point, with 0.5 nm step, 1 nm bandwidth, and 1 s collection time per step, taking three averages. The post-acquisition smoothing tool of the Chirascan software was used to remove random noise elements from the averaged spectra. A residual plot was generated for each curve to verify whether or not the spectrum was distorted during the smoothing process. Following background (water) correction, the CD data were normalized to molar mean residue ellipticity.

The absorbance and CD spectra were cutoff at 200 nm as both hydrolyzed GdL and HCl absorb below 200 nm. GdL displays a CD signal at 218 nm. Its hydrolysis product (gluconic acid) is CD silent above 200 nm (Figure S1).

Transmission Electron Microscopy. TEM experiments were performed using a Philips CM20 transmission electron microscope operated at 200 kV. One drop of peptide solution was placed on the shiny side of 300 mesh Cu grids coated with a carbon film (Agar Scientific, UK) for 1 min. The excess solution at the sides of the grid was cleaned carefully. The shiny side of the grid was placed over a drop of aqueous uranyl acetate (1 wt %) (Agar Scientific, UK) for 1 min. The excess solution at the sides of the grid was cleaned very carefully. The grid was then allowed to dry at room temperature. Peptide solutions, five-times more diluted than the critical gelation concentration (CGC), were used for TEM. Peptide solutions for TEM were prepared in a solvent system similar to that used to prepare the gels. Npx-L-Trp-*Z*-ΔPhe-OH (**7a**): 0.080 wt % (1.42 mM) in H_2O, NaOH 1 M [1.62% (v/v)] and GdL (0.44 wt %), final pH 6.07; Npx-L-Trp-*Z*-ΔAbu−OH (**7b**): 0.080 wt % (1.60 mM) in H_2O, NaOH 1 M [0.95% (v/v)] and GdL (0.23 wt %), final pH 5.65; Npx-L-Trp-ΔAla-OH (**7c**) with GdL: 0.120 wt % (2.47 mM) in H_2O, NaOH 1 M [1.13% (v/v)] and GdL (0.25 wt %), final pH 6.40; Npx-L-Trp-ΔAla-OH (**7c**) with HCl: 0.117 wt % (2.41 mM) in H_2O, NaOH 1 M [2.5% (v/v)] and HCl 0.1 M [5.5% (v/v)], final pH 6.26.

TEM and CD experiments were carried out using peptide solutions prepared in identical conditions, similar peptide and GdL (HCl) concentration, and pH.

Rheology. Rheology experiments were carried out using a PaarPhysica MCR300 rheometer, equipped with a TEK 350-C plate with TC20/EDT/TEK temperature control and a cylindrical plunger with a diameter of 10 mm. The hydrogels were prepared in soda glass specimen tubes (Samco, UK), which also served as cup for the rheological measurements. The vials had diameters of 25 mm, and the measurements were performed until a gap of 1.5 mm to the bottom of the vials was reached to avoid significant end effects. The normal force was measured as a function of penetration distance in the gel. Young's moduli were computed neglecting any plunger buoyancy effect, following the approach of Oakenfull et al.[31] The slope and associated standard error of the linear regime of the stress−strain response curves (Young's moduli) were determined using the OriginPro 8 software.

DOI: 10.1021/acs.biomac.5b01006
Biomacromolecules 2015, 16, 3562−3573

Strain and stress at break correspond to the location of the first maximum in the stress−strain curves.

Spectroscopic Measurements. Fluorescence measurements were performed using a Fluorolog 3 spectrofluorimeter, equipped with double monochromators in both excitation and emission, Glan-Thompson polarizers, and a temperature controlled cuvette holder. Fluorescence emission and excitation spectra were corrected for the instrumental response of the system.

Förster Resonance Energy Transfer Measurements. A stock solution of compound **8** in ethanol (5×10^{-4} M) was added to the solution of hydrogelator **7a** during the gelation process, keeping the ethanol content lower than 1%. The final concentration of compound **8** was 3×10^{-6} M. The interaction of the potential antitumor drug with the hydrogel was investigated by Förster resonance energy transfer (FRET). FRET efficiency, Φ_{RET}, defined as the fraction of donor molecules that have transferred their excess energy to acceptor molecules, can be obtained by taking the ratio of the donor integrated fluorescence intensities (with respect to wavenumber) in the presence of acceptor (F_{DA}) and in the absence of acceptor (F_D) (eq 1):[32]

$$\Phi_{RET} = 1 - \frac{F_{DA}}{F_D} \tag{1}$$

The distance between donor and acceptor molecules can be determined through the FRET efficiency (eq 2), where R_0 is the Förster radius (critical distance) that can be obtained by the spectral overlap, $J(\lambda)$, between the donor emission and the acceptor absorption according to eqs 3 and 4 (with R_0 in Å, λ in nm, $\varepsilon_A(\lambda)$ in M^{-1} cm^{-1}),[32] where $k^2 = {}^2/_3$ is the orientational factor assuming random orientation of the dyes, Φ_D^0 is the fluorescence quantum yield of the donor in the absence of energy transfer, n is the refraction index of the medium, $I_D(\lambda)$ is the fluorescence spectrum of the donor normalized so that $\int_0^\infty I_D(\lambda)\, d\lambda = 1$, and $\varepsilon_A(\lambda)$ is the molar absorption coefficient of the acceptor:

$$r_{AD} = R_0 \left[\frac{1 - \Phi_{RET}}{\Phi_{RET}} \right]^{1/6} \tag{2}$$

$$R_0 = 0.2108[k^2 \Phi_D^0 n^{-4} J(\lambda)]^{1/6} \tag{3}$$

$$J(\lambda) = \int_0^\infty I_D(\lambda)\varepsilon_A(\lambda)\lambda^4\, d\lambda \tag{4}$$

The fluorescence quantum yield, Φ_s, of the energy donor was determined by the standard method (eq 5),[33,34] where A is the absorbance at the excitation wavelength, F the integrated emission area, and n is the refraction index of the solvents. Subscripts refer to the reference (r) or sample (s) compound. The absorbance value at excitation wavelength was always less than 0.1 to avoid inner filter effects. L-Trp in aqueous buffer solution (pH = 7.2) was used as reference (Φ_R = 0.14 at 25 °C):[35]

$$\Phi_s = [(A_r F_s n_s^2)/(A_s F_r n_r^2)]\Phi_r \tag{5}$$

Synthesis. Compounds **1** (CAS 13139−14−5), **2b** (CAS 39994−75−7), and **3c** (CAS 81187−76−0) are commercially available.

Synthesis of Boc-L-Trp-OH (1). A solution of H-L-Trp-OH (1.25 g, 6.12 mmol) in 1,4-dioxane (12 mL), distilled water (6 mL), and NaOH 1 M (6 mL) was put in an ice bath. Di-*tert*-butyl dicarbonate (1.10 equiv, 1.47 g, 6.73 mmol) was added, and the mixture was left stirring at room temperature (rt) for 1 h. The aqueous solvents were removed under reduced pressure, and then the solution was acidified to pH 2−3 with an aqueous solution of $KHSO_4$ 1 M. The aqueous phase was extracted with ethyl acetate (3 × 30 mL). The organic phases were gathered together, washed with distilled water (2 × 30 mL), dried over magnesium sulfate anhydrous, and the solvent removed under reduced pressure, giving compound **1** (1.70 g, 91%) as a white solid; mp: 133.0−135.0 °C (mp_{lit}: 134−139 °C); ^{1}H NMR (400 MHz, DMSO-d_6, δ): 1.31 (s, 9H, 3 × CH_3), 2.96 (dd, J = 9.2 and 14.4 Hz, 1H, βCH), 3.11 (dd, J = 4.8 and 14.4 Hz, 1H, βCH), 4.13 (ddd, J = 4.8, 9.2, and 12.8 Hz, 1H, αCH), 6.93−6.99 (m, 2H, Ar H and NH), 7.05 (dt, J = 1.0 and 8.0 Hz, 1H, Ar H), 7.13 (d, J = 2.0 Hz, 1H, Ar H), 7.32 (d, J = 8.0 Hz, 1H, Ar H), 7.50 (d, J = 8.0 Hz, 1H, Ar H), 10.81 (s, 1H, NH), 12.50 (brs, 1H, CO_2H).

Synthesis of Amino Acid Methyl Esters Hydrochlorides (2a−c). To methanol (1 mL $mmol^{-1}$ of amino acid) in an ice bath was slowly added thionyl chloride (3.40 equiv). The amino acid was added slowly, and the mixture was left stirring at 40 °C for 4 h. The solvent was removed under reduced pressure, and ethyl ether was added. The mixture was stored in the freezer for 1 h, and then the solid was filtered.

H-D,L-Phe(β−OH)-OMe,HCl (2a). H-D,L-Phe(β−OH)−OH (8.40 g, 46.6 mmol) gave compound **2a** as a white solid (10.40 g, 97%); mp: 145.0−146.0 °C; ^{1}H NMR (300 MHz, $CDCl_3$, δ): 3.59 (s, 3H, OCH_3), 4.13 (brs, 1H, CH), 5.01 (d, J = 5.4 Hz, 1H, CH), 7.31−7.38 (m, 5H, Ar H), 8.53 (brs, 3H, NH_3^+).

H-D,L-Thr-OMe,HCl (2b). H-D,L-Thr-OH (11.91 g, 100 mmol) gave compound **2b** as an oil (16.90 g, quant); ^{1}H NMR (300 MHz, DMSO-d_6, δ): 1.18 (d, J = 6.6 Hz, 3H, γCH_3), 3.71 (s, 3H, OCH_3), 3.89 (t, J = 4.2 Hz, 1H, αCH), 4.06−4.14 (m, 1H, βCH), 5.34 (s, 1H, OH), 8.49 (s, 3H, NH_3^+).

H-D,L-Ser-OMe,HCl (2c):[36] H-D,L-Ser-OH (10.6 g, 100 mmol) gave compound **2c** as a white solid (15.6 g, quant); mp: 163.0−165.0 °C (mp_{lit}: 165−166 °C); ^{1}H NMR (300 MHz, DMSO-d_6, δ): 3.74 (s, 3H, OCH_3), 3.81 (d, J = 3.6 Hz, 2H, βCH_2), 4.10 (brs, 1H, αCH), 5.58 (brs, 1H, OH), 8.55 (brs, 3H, NH_3^+).

Synthesis of *N*-Boc-Dipeptides (3a−c). Boc-L-Trp-OH (**1**) was dissolved in acetonitrile (10 mL $mmol^{-1}$) and put in an ice bath. HOBt (1.00 equiv), DCC (1.00 equiv), amino acid methyl ester (1.00 equiv), and triethylamine (2.00 equiv) were added with about 2 min between each addition. The mixture was left stirring at rt overnight (~18 h). The urea was filtered and the solvent removed under reduced pressure. Acetone was added, and the mixture was stored in the freezer for 2 h. The urea was filtered again. Evaporation at reduced pressure gave a residue that was partitioned between ethyl acetate (50 mL) and $KHSO_4$ (30 mL, 1 M). The organic phase was thoroughly washed with $KHSO_4$ (1 M), $NaHCO_3$ (1 M), and brine (3 × 30 mL, each) and dried with $MgSO_4$. Removal of the solvent afforded compounds **3a−c**.

Boc-L-Trp-D,L-Phe(β−OH)-OMe (3a). Boc-L-Trp-OH (**1**) (0.70 g; 2.30 mmol) and H-D,L-Phe(β−OH)-OMe,HCl (**2a**) gave compound **3a** as a light yellow foam (1.00 g, 90%); ^{1}H NMR (400 MHz, $CDCl_3$, δ): 1.40 (s, 18H, 6 × CH_3), 3.09−3.15 (m, 4H, 2 × βCH_2), 3.63 (s, 6H, 2 × OCH_3), 4.46 (brs, 2H, 2 × αCH Trp), 4.77 (brs, 1H, αCH), 4.81−4.84 (m, 1H, αCH), 5.11 (brs, 4H, 2 × βCH, 2 × NH), 6.76 (brs, 2H, Ar H, NH), 6.90 (d, J = 8.8 Hz, 1H, NH), 6.96 (brs, 1H, Ar H), 7.08−7.14 (m, 2H, Ar H), 7.16−7.21 (m, 4H, Ar H), 7.23−7.29 (m, 8H, Ar H), 7.33 (t, J = 7.2 Hz, 2H, Ar H), 7.55 (d, J = 7.6 Hz, 1H, Ar H), 7.63 (d, J = 8.0 Hz, 1H, Ar H), 8.24 (s, 1H, 1-NH), 8.30 (s, 1H, 1-NH); ^{13}C NMR (100.6 MHz, $CDCl_3$, δ): 27.98 (βCH_2), 28.10 (βCH_2), 28.21 (6 × CH_3), 52.44 (CH_3), 52.52 (CH_3), 54.86 (αCH), 55.08 (αCH), 58.34 (αCH), 58.36 (αCH), 73.66 (βCH), 73.81 (βCH), 80.16 (2 × C), 110.11 (C-3), 110.30 (C-3), 111.17 (2 × CH), 118.69 (CH), 118.73 (CH), 119.55 (CH), 119.61 (CH), 122.05 (CH), 122.10 (CH), 123.07 (CH), 123.33 (CH), 125.86 (4 × C_o), 127.45 (C-3a), 127.59 (C-3a), 127.99 (C_p), 128.08 (C_p), 128.30 (2 × C_m), 128.41 (2 × C_m), 136.10 (C-7a), 136.18 (C-7a), 139.41 (C_i), 139.46 (C_i), 155.52 (2 × C═O), 170.68 (C═O), 170.39 (C═O), 172.06 (C═O), 172.12 (C═O); HRMS (ESI) m/z: $[M + H]^+$ calcd for $C_{26}H_{32}N_3O_6^+$, 482.2285; found, 482.2283.

Boc-L-Trp-D,L-Thr-OMe (3b). Boc-L-Trp-OH (**1**) (0.91 g; 3.00 mmol) and H-D,L-Thr-OMe,HCl (**2b**) gave compound **3b** as a white foam (1.24 g, 99%); ^{1}H NMR (400 MHz, $CDCl_3$, δ): 1.08 (d, J = 5.6 Hz, 3H, CH_3), 1.42 (s, 9H, 3 × CH_3), 3.26 (d, J = 5.2 Hz, 2H, βCH_2), 3.66 (s, 3H, OCH_3), 4.21 (dq, J = 3.2 and 6.4 Hz, 1H, βCH), 4.50−4.53 (m, 2H, 2 × αCH), 5.26 (d, J = 7.6 Hz, 1H, NH), 6.75 (d, J = 7.6 Hz, 1H, NH), 7.10 (s, 1H, H-2), 7.11 (dt, J = 1.2 and 8.0 Hz, 1H, H-5), 7.18 (dt, J = 1.2 and 8.0 Hz, 1H, H-6), 7.34 (d, J = 8.0 Hz, 1H, H-7), 7.64 (d, J = 8.0 Hz, 1H, H-4), 8.30 (s, 1H, 1-NH); ^{13}C NMR (100.6 MHz, $CDCl_3$, δ): 19.71 (CH_3), 27.94 (βCH_2), 28.24 (3 × CH_3), 52.46 (OCH_3), 55.42 (αCH), 57.46 (αCH), 68.22 (βCH), 80.27 (C), 110.35 (C-3), 111.16 (CH-7), 118.75 (CH-4), 119.61

DOI: 10.1021/acs.biomac.5b01006
Biomacromolecules 2015, 16, 3562−3573

(CH-5), 122.12 (CH-6), 123.29 (CH-2), 127.53 (C-3a), 136.20 (C-7a), 155.64 (C═O), 170.96 (C═O), 172.34 (C═O); Anal. Calcd for $C_{21}H_{29}N_3O_6$, C 60.13, H 6.97, N 10.02; found, C 60.23, H 6.84, N 10.01.

Boc-L-Trp-D,L-Ser-OMe (3c). Boc-L-Trp-OH (**1**) (0.91 g, 2.99 mmol) and H-D,L-Ser-OMe,HCl (**2c**) gave compound **3c** as a colorless oil that spontaneously crystallized (0.97 g, 80%); ^{1}H NMR (400 MHz, $CDCl_3$, δ): 1.42 (s, 9H, 3 × CH_3), 2.42 (brs, 1H, OH), 3.21 (dd, J = 6.8 and 14.8 Hz, 1H, βCH Trp), 3.37 (dd, J = 6.0 and 14.8 Hz, 1H, βCH Trp), 3.70 (s, 3H, OCH_3), 3.79−3.82 (m, 2H, βCH_2 Ser), 4.42−4.44 (m, 1H, αCH), 4.50−4.52 (m, 1H, αCH), 5.19 (d, J = 4.4 Hz, 1H, NH), 6.87 (d, J = 6.9 Hz, 1H, NH), 7.08−7.21 (m, 2H, Ar H), 7.27 (s, 1H, Ar H), 7.34 (d, J = 7.8 Hz, 1H, Ar H), 7.62 (d, J = 7.5 Hz, 1H, Ar H), 8.51 (brs, 1H, NH).

Synthesis of Dehydrodipeptide Derivatives (4a and 4c). DMAP (0.1 equiv) was added to solutions of compounds **3a−c** in dry acetonitrile (1 M) followed by Boc_2O (1.0 equiv) under rapid stirring at rt. The reaction was monitored by ^{1}H NMR until all the reactant had been consumed (18−24 h). Then *N,N,N′,N′*-tetramethylguadinine (2% in volume) was added, stirring was continued, and the reaction followed by ^{1}H NMR. When all the reactant had been consumed (5−7 h), evaporation at reduced pressure gave a residue that was partitioned between ethyl acetate (50 mL) and $KHSO_4$ (30 mL, 1 M). The organic phase was thoroughly washed with $KHSO_4$ (1 M), $NaHCO_3$ (1 M), and brine (3 × 30 mL, each) and dried with $MgSO_4$. Removal of the solvent afforded compounds **4a−c**.

Boc-L-Trp-Z-ΔPhe-OMe (4a). Boc-L-Trp-D,L-Phe(β−OH)-OMe (**3a**) (0.81 g, 1.68 mmol) gave compound **4a** as a light yellow foam (0.70 g, 90%); mp: 135.0−137.0 °C; ^{1}H NMR (400 MHz, $CDCl_3$, δ): 1.42 (s, 9H, 3 × CH_3), 3.31 (d, J = 6.0 Hz, 2H, βCH_2), 3.78 (s, 3H, OCH_3), 4.63 (d, J = 5.6 Hz, 1H, αCH), 5.11 (brs, 1H, NH), 7.11 (s, 1H, H-2), 7.14 (dt, J = 1.0 and 8.0 Hz, 1H, H-5), 7.22 (dt, J = 1.0 and 8.0 Hz, 1H, H-6), 7.26−7.28 (m, 5H, Ar H), 7.34 (s, 1H, βCH), 7.37 (d, J = 8.0 Hz, 1H, H-7), 7.64 (brs, 1H, NH), 7.66 (d, J = 8.0 Hz, 1H, H-4), 8.24 (brs, 1H, 1-NH); ^{13}C NMR (100.6 MHz, $CDCl_3$, δ): 27.44 (βCH_2), 28.25 (3 × CH_3), 52.57 (OCH_3), 55.41 (αCH), 80.38 (C), 110.14 (C-3), 111.22 (CH-7), 118.72 (CH-4), 119.77 (CH-5), 122.22 (CH-6), 123.54 (CH-2), 123.88 (αC), 127.50 (C-3a), 128.54 (CH_m), 129.39 (CH_p), 129.67 (CH_o), 132.36 (βCH), 133.42 (C_i), 136.21 (C-7a), 155.68 (C═O), 165.33 (C═O), 172.63 (C═O); HRMS (ESI) m/z: $[M + H]^+$ calcd for $C_{26}H_{30}N_3O_5^+$, 464.2180; found, 464.2178.

Boc-L-Trp-ΔAla-OMe (4c). Boc-L-Trp-D,L-Ser-OMe (**3c**) (0.67 g, 1.65 mmol) gave compound **4c** as an oil that crystallized (0.55 g, 86%); mp: 62.0−64.0 °C (mp_{lit}: 78−80 °C[37]); ^{1}H NMR (300 MHz, $CDCl_3$, δ): 1.43 (s, 9H, 3 × CH_3), 3.21−3−35 (m, 2H, βCH_2), 3.73 (s, 3H, OCH_3), 4.53 (brs, 1H, αCH), 5.13 (brs, 1H, NH), 5.87 (s, 1H, βCH), 6.61 (s, 1H, βCH), 7.06 (d, J = 2.1 Hz, 1H, H-2), 7.12 (dt, J = 1.2 and 6.9 Hz, 1H, H-5), 7.21 (dt, J = 0.9 and 6.9 Hz, 1H, H-6), 7.37 (d, J = 7.7 Hz, 1H, H-7), 7.62 (d, J = 7.8 Hz, 1H, H-4), 8.13 (brs, 1H, NH), 8.21 (brs, 1H, NH); ^{13}C NMR (75.4 MHz, $CDCl_3$, δ): 28.16 (βCH_2), 28.21 (3 × CH_3), 52.80 (OCH_3), 55.91 (αCH), 80.42 (C), 109.20 (βCH_2), 110.21 (C-3), 111.17 (CH-7), 118.75 (CH-4), 119.80 (CH-5), 122.30 (CH-6), 123.08 (CH-2), 127.35 (C-3a), 130.62 (αC), 133.23 (C-7a), 155.45 (C═O Boc), 163.89 (C═O ΔAla), 170.72 (C═O Trp).

Synthesis of Dehydrodipeptide Derivatives (4bi and 4bii). DMAP (0.1 equiv) was added to a solution of compound **3b** (1.86 g; 4.43 mmol) in dry acetonitrile (1 M) followed by Boc_2O (1.0 equiv) under rapid stirring at rt. The reaction was monitored by ^{1}H NMR until all the reactant had been consumed. After 3 days, more Boc_2O (0.5 equiv) and DMAP (0.05 equiv) were added, and the mixture was left stirring for 1 more day. Then *N,N,N′,N′*-tetramethylguadinine (4% in volume) was added, stirring was continued, and the reaction followed by ^{1}H NMR. When all the reactant had been consumed (8 h), evaporation at reduced pressure gave a residue that was partitioned between ethyl acetate (50 mL) and $KHSO_4$ (30 mL, 1 M). The organic phase was thoroughly washed with $KHSO_4$ (1 M), $NaHCO_3$ (1 M) and brine (3 × 30 mL, each) and dried with $MgSO_4$. Removal of the solvent afforded a yellow oil (1.43 g), which was applied to a dry flash chromatography (petroleum ether/ethyl acetate, mixtures of crescent polarity).

Boc-L-Trp-Z-ΔAbu-OMe (4bi). Compound **4bi** was obtained as a white solid (0.55 g, 31%); mp: 135.0−137.0 °C; ^{1}H NMR (400 MHz, $CDCl_3$, δ): 1.43 (s, 9H, 3 × CH_3), 1.66 (d, J = 7.2 Hz, 3H, γCH_3), 3.31 (d, J = 6.0 Hz, 2H, βCH_2), 3.69 (s, 3H, OCH_3), 4.60 (brs, 1H, αCH), 5.19 (brs, 1H, NH), 6.76 (q, J = 7.2 Hz, 1H, βCH), 7.12 (brs, 1H, H-2 Trp), 7.13 (dt, J = 0.8 and 7.4 Hz, 1H, Ar H), 7.21 (dt, J = 1.2 and 7.6 Hz, 1H, Ar H), 7.34 (brs, 1H, NH ΔAbu), 7.36 (d, J = 8.4 Hz, 1H, Ar H), 7.67 (d, J = 8.0 Hz, 1H, Ar H), 8.27 (s, 1H, NH-1 Trp); ^{13}C NMR (100.6 MHz, $CDCl_3$, δ): 14.45 (γCH_3), 27.87 (βCH_2), 28.24 (3 × CH_3), 52.22 (OCH_3), 55.36 (αCH), 80.30 (C), 110.28 (C), 111.19 (CH), 118.80 (CH), 119.73 (CH), 122.22 (CH), 123.39 (H-2 Trp), 125.79 (αC), 127.49 (C), 134.37 (βCH), 136.23 (C), 155.58 (C═O), 164.60 (C═O), 170.20 (C═O); HMRS (ESI) m/z: $[M + H]^+$ calcd for $C_{21}H_{28}N_3O_5^+$, 402.2024; found, 402.2023.

Boc-L-Trp(N-Boc)-Z-ΔAbu-OMe (4bii). Compound **4bii** was obtained as an colorless oil that spontaneously crystallized (0.54 g, 24%); mp: 82.0−83.0 °C; ^{1}H NMR (400 MHz, $CDCl_3$, δ): 1.43 (s, 9H, 3 × CH_3), 1.66 (s, 9H, 3 × CH_3), 1.68 (d, J = 7.2 Hz, 3H, γCH_3), 3.20−3.30 (m, 2H, βCH_2), 3.70 (s, 3H, OCH_3), 4.59 (brs, 1H, αCH), 5.15 (brs, 1H, NH), 6.79 (q, J = 7.2 Hz, 1H, βCH), 7.25 (dt, J = 0.8 and 7.2 Hz, 1H, Ar H), 7.33 (dt, J = 1.2 and 8.4 Hz, 1H, Ar H), 7.35 (brs, 1H, NH ΔAbu), 7.49 (s, 1H, H-2 Trp), 7.63 (d, J = 7.6 Hz, 1H, Ar H), 8.15 (d, J = 7.6 Hz, 1H, Ar H); ^{13}C NMR (100.6 MHz, $CDCl_3$, δ): 14.54 (γCH_3), 27.90 (βCH_2), 28.16 (3 × CH_3), 28.22 (3 × CH_3), 52.25 (OCH_3), 54.72 (αCH), 80.47 (C), 83.59 (C), 119.03 (C), 115.26 (CH), 124.41 (CH), 124.61 (CH), 130.21 (CH), 135.54 (H-2 Trp), 125.67 (αC), 122.71 (C), 134.43 (βCH), 130.21 (C), 149.50 (C═O), 155.47 (C═O), 164.48 (C═O), 169.61 (C═O); HMRS (ESI) m/z: $[M + H]^+$ calcd for $C_{26}H_{36}N_3O_7^+$, 502.2548; found, 502.2551.

Synthesis of *N*-Deprotected Dehydropeptides Derivatives (5a−c). TFA (3 mL $mmol^{-1}$) was added to the *N*-Boc-peptide, and the mixture was left stirring at rt. The reaction was followed by TLC (ethyl ether). When no starting material was observed, the solvent was removed under reduced pressure. Diethyl ether was added, and the solvent removed again under reduced pressure. Precipitation from ethyl ether or petroleum ether afforded compounds **5a−c**.

H-L-Trp-Z-ΔPhe-OMe,TFA (5a). Boc-L-Trp-*Z*-ΔPhe-OMe (**4a**) (0.51 g, 1.10 mol) gave compound **5a** as a cream solid (0.46 g, 87%); mp: 115.0−117.0 °C; ^{1}H NMR (400 MHz, DMSO-d_6, δ): 3.08−3.14 (m, 1H, βCH), 3.39−3.43 (m, 1H, βCH), 3.74 (s, 3H, OCH_3), 4.21−4.32 (m, 1H, αCH), 7.02 (dt, J = 0.8 and 7.6 Hz, 1H, Ar H), 7.11 (dt, J = 0.8 and 7.6 Hz, 1H, Ar H), 7.27 (d, J = 2.4 Hz, 1H, Ar H), 7.34−7.40 (m, 6H, βCH and Ar H), 7.59−7.61 (m, 2H, Ar H), 7.76 (d, J = 7.6 Hz, 1H, Ar H), 8.19 (s, 3H, NH_3^+), 10.45 (s, 1H, NH), 11.08 (d, J = 2.0 Hz, 1H, NH); ^{13}C NMR (100.6 MHz, DMSO-d_6, δ): 27.26 (βCH), 52.37 (OCH_3), 52.68 (αCH), 106.69 (C), 111.56 (CH), 118.47 (CH), 118.54 (CH), 121.25 (CH), 125.16 (αC), 125.19 (CH), 126.99 (C), 128.67 (CH), 129.70 (CH), 130.03 (CH), 132.53 (βCH), 132.91 (C), 136.42 (C), 164.94 (C═O ΔPhe), 168.82 (C═O Trp); HRMS (ESI) m/z: $[M]^+$ calcd for $C_{21}H_{22}N_3O_3^+$, 364.1656; found, 364.1655.

H-L-Trp-Z-ΔAbu-OMe,TFA (5b). Boc-L-Trp-*Z*-ΔAbu-OMe (**4bi**) (0.18 g; 0.45 mol) gave compound **5b** as a cream solid (89 mg, 47%). Boc-L-Trp(*N*-Boc)-*Z*-ΔAbu-OMe (**4bii**) (0.23 g; 0.46 mol) gave compound **5b** as a cream solid (0.17 g, 89%); mp: 111.0−113.0 °C; ^{1}H NMR (400 MHz, DMSO-d_6, δ): 1.63 (d, J = 7.2 Hz, 3H, γCH_3), 3.12 (dd, J = 8.8 and 14.8 Hz, 1H, βCH), 3.33 (dd, J = 5.6 and 14.8 Hz, 1H, βCH), 3.67 (s, 3H, OCH_3), 4.15 (brs, 1H, αCH), 6.64 (q, J = 7.2 Hz, 1H, βCH), 7.02 (dt, J = 0.8 and 8.0 Hz, 1H, H-5 Trp), 7.10 (dt, J = 0.8 and 7.2 Hz, 1H, H-6 Trp), 7.25 (d, J = 2.0 Hz, 1H, H-2 Trp), 7.37 (d, J = 8.4 Hz, 1H, H-7 Trp), 7.73 (d, J = 7.6 Hz, 1H, H-4 Trp), 8.16 (brs, 3H, NH_3^+), 9.94 (s, 1H, NH ΔAbu), 11.04 (s, 1H, NH Trp); ^{13}C NMR (100.6 MHz, DMSO-d_6, δ): 13.50 (γCH_3), 27.51 (βCH_2), 52.02 (OCH_3), 52.70 (αCH), 106.69 (C-3 Trp), 111.50 (CH-7 Trp), 118.45 (CH-4 or CH-5 Trp), 118.49 (CH-4 or CH-5 Trp), 121.20 (CH-6 Trp), 125.07 (CH-2 Trp), 126.76 (αC), 127.01 (C-3a Trp), 133.84 (βCH), 136.33 (C-7a Trp), 164.16 (C═O

DOI: 10.1021/acs.biomac.5b01006
Biomacromolecules 2015, 16, 3562−3573

ΔAbu), 167.77 (C═O Trp); HRMS (ESI) *m/z*: $[M]^+$ calcd for $C_{16}H_{20}N_3O_3^+$, 302.1499; found, 302.1500.

*H-L-Trp-ΔAla-OMe,TFA (**5c**).* Boc-L-Trp-ΔAla-OMe (**4c**) (0.13 g, 0.34 mol) gave compound **5c** as a yellow solid (66 mg, 51%); mp: *deg* > 140.0 °C; ^{1}H NMR (300 MHz, DMSO-d_6, δ): 3.13−3.28 (m, 2H, βCH_2), 3.75 (s, 3H, OCH_3), 4.35 (brs, 1H, αCH), 5.84 (s, 1H, βCH), 6.22 (s, 1H, βCH), 6.98 (dt, *J* = 0.9 and 7.5 Hz, 1H, Ar H), 7.08 (dt, *J* = 1.2 and 7.2 Hz, 1H, Ar H), 7.21 (d, *J* = 2.4 Hz, 1H, H-2 Trp), 7.36 (d, *J* = 7.4 Hz, 1H, Ar H), 7.62 (d, *J* = 8.1 Hz, 1H, Ar H), 8.19 (brs, 3H, NH_3^+), 9.98 (s, 1H, NH), 11.03 (s, 1H, NH Trp); ^{13}C NMR (75.4 MHz, DMSO-d_6, δ): 27.30 (βCH_2), 52.76 (OCH_3), 52.98 (αCH), 106.49 (C), 111.47 (CH), 111.63 (βCH), 118.45 (2 × CH), 121.18 (CH), 125.03 (CH), 127.04 (C), 136.26 (C), 132.03 (αC), 163.42 (C═O ΔAla), 168.54 (C═O Trp); HMRS (ESI) *m/z*: $[M + H]^{2+}$ $C_{15}H_{18}N_3O_3^{2+}$ requires 288.1343; found, 288.1342.

Synthesis of (*S*)-(+)-Naproxen Dehydrodipeptides (6a−c). The methyl ester of the peptide (1.10 equiv) was dissolved in DCM (5 mL mmol^{-1}) and put in an ice bath. Triethylamine (2.20 equiv) was added and, slowly, (*S*)-(+)-naproxen chloride. The mixture was left stirring at rt overnight (∼18 h). The mixture was filtered. Evaporation at reduced pressure gave a residue that was partitioned between ethyl acetate (50 mL) and $KHSO_4$ (30 mL, 1 M). The organic phase was thoroughly washed with $KHSO_4$ (1 M), $NaHCO_3$ (1 M), and brine (3 × 30 mL, each) and dried with $MgSO_4$. Removal of the solvent afforded compounds **6a−c**.

*Npx-L-Trp-Z-ΔPhe-OMe (**6a**).* H-L-Trp-Z-ΔPhe-OMe,TFA (**5a**) (0.30 g, 0.63 mmol) gave compound **6a** from a column chromatography (ethyl ether) as a white solid (0.14 g, 39%); mp: 211.0−213.0 °C; ^{1}H NMR (400 MHz, DMSO-d_6, δ): 1.26 (d, *J* = 7.2 Hz, 3H, CH_3 Npx), 2.99 (dd, *J* = 9.0 and 14.4 Hz, 1H, βCH), 3.22 (dd, *J* = 5.2 and 14.4 Hz, 1H, βCH), 3.58 (s, 3H, OCH_3), 3.84 (s, 3H, OCH_3 Npx), 3.79−3.85 (m, 1H, CH Npx), 4.77−4.83 (m, 1H, αCH), 6.99 (dt, *J* = 0.8 and 7.2 Hz, 1H, Ar H Trp), 7.06−7.19 (m, 6H, βCH, Ar H), 7.20 (d, *J* = 2.0 Hz, 1H, H-2 Trp), 7.23 (d, *J* = 2.8 Hz, 1H, Ar H Npx), 7.35 (d, *J* = 8.4 Hz, 1H, Ar H Trp), 7.40 (dd, *J* = 1.6 and 8.8 Hz, 1H, Ar H Npx), 7.48 (d, *J* = 6.4 Hz, 1H, Ar H Npx), 7.66−7.70 (m, 5H, Ar H), 8.30 (d, *J* = 8.4 Hz, 1H, NH), 9.82 (s, 1H, NH), 10.85 (d, *J* = 1.6 Hz, 1H, NH); ^{13}C NMR (100.6 MHz, DMSO-d_6, δ): 18.85 (CH_3 Npx), 27.68 (βCH_2), 44.53 (CH Npx), 52.00 (OCH_3), 53.17 (αCH), 55.09 (OCH_3 Npx), 105.61 (CH Npx), 109.92 (C-3 Trp), 111.23 (CH Trp), 118.18 (CH Trp), 118.38 (CH), 118.54 (CH), 120.84 (CH), 123.72 (CH-2 Trp), 125.33 (CH Npx), 125.83 (C), 126.38 (CH ΔPhe), 126.61 (CH Npx), 127.36 (C-3a Trp), 128.31 (C), 128.37 (CH ΔPhe), 129.01 (CH ΔPhe), 129.19 (CH Npx), 129.92 (CH Npx), 131.89 (CH Npx), 133.04 (C), 133.10 (C), 136.05 (C-7a Trp), 137.26 (C-2 Npx), 156.88 (C-6 Npx), 165.33 (C═O), 171.60 (C═O Trp), 173.30 (C═O Npx); HRMS (ESI) *m/z*: $[M + H]^+$ calcd for $C_{35}H_{34}N_3O_5^+$, 576.2493; found, 576.2498.

*Npx-L-Trp-Z-ΔAbu-OMe (**6b**).* H-L-Trp-Z-ΔAbu-OMe,TFA (**5b**) (0.57 g, 1.37 mmol) gave compound **6b** from a dry column chromatography (petroleum ether/ethyl acetate, 1:1) as a white solid (0.37 mg, 53%); mp: 180.0−182.0 °C; ^{1}H NMR (400 MHz, $CDCl_3$, δ): 1.51 (d, *J* = 7.2 Hz, 3H, CH_3 ΔAbu), 1.55 (d, *J* = 7.2 Hz, 3H, CH_3 Npx), 3.22−3.24 (m, 2H, βCH_2), 3.60 (s, 3H, OCH_3 ΔAbu), 3.61 (q, *J* = 7.2 Hz, 1H, CH), 3.92 (s, 3H, OCH_3 Npx), 4.86 (q, *J* = 7.2 Hz, 1H, αCH), 6.19 (d, *J* = 7.2 Hz, 1H, NH Trp), 6.67 (q, *J* = 7.2 Hz, 1H, βCH), 6.84 (d, *J* = 2.4 Hz, 1H, H-2 Trp), 7.07−7.08 (m, 1H, Ar H Npx), 7.10 (dt, *J* = 0.8 and 8.0 Hz, 1H, H-5 Trp), 7.14 (dd, *J* = 2.8 and 8.8 Hz, 1H, Ar H Npx), 7.19 (dt, *J* = 1.2 and 8.0 Hz, 1H, CH-6 Trp), 7.22 (dd, *J* = 1.6 and 8.0 Hz, 1H, Ar H Npx), 7.31 (d, *J* = 8.0 Hz, 1H, H-7 Trp), 7.35 (s, 1H, NH ΔAbu), 7.48 (d, *J* = 0.8 Hz, 1H, H-1 Npx), 7.58−7.61 (m, 2H, Ar H Npx), 7.62 (d, *J* = 7.6 Hz, 1H, CH-4 Trp), 8.02 (s, 1H, NH-1 Trp); ^{13}C NMR (100.6 MHz, $CDCl_3$, δ): 14.17 (CH_3 ΔAbu), 17.99 (CH_3 Npx), 27.12 (βCH_2), 46.87 (CH), 52.12 (OCH_3 ΔAbu), 53.76 (αCH), 55.30 (OCH_3 Npx), 105.55 (CH Npx), 110.00 (C-3 Trp), 111.20 (CH-7 Trp), 118.66 (CH-4 Trp), 119.01 (CH Npx), 119.72 (CH-5 Trp), 122.18 (CH-6 Trp), 123.27 (CH-2 Trp), 125.83 (αC), 125.91 (CH Npx), 126.06 (CH-1 Npx), 127.35 (C-3a Trp), 127.49 (CH Npx), 128.91 (C Npx), 129.28 (CH Npx), 133.70 (C Npx), 134.40 (βCH), 135.65 (C-2 Npx), 136.11 (C-7a Trp), 157.70 (C-6 Npx), 164.46 (C═O ΔAbu), 169.79 (C═O Trp), 174.82 (C═O Npx); HRMS (ESI) *m/z*: $[M + H]^+$ calcd for $C_{30}H_{32}N_3O_5^+$, 514.2336; found, 514.2335.

*Npx-L-Trp-ΔAla-OMe (**6c**).* H-L-Trp-ΔAla-OMe,TFA (**5c**) (0.40 g, 1.00 mmol) gave compound **6c** from a column chromatography (petroleum ether: ethyl ether, mixtures of crescent polarity) as a white solid (0.15 g, 30%); mp: 145.0−147.0 °C; ^{1}H NMR (400 MHz, $CDCl_3$, δ): 1.61 (d, *J* = 7.2 Hz, 3H, CH_3), 3.09 (dd, *J* = 7.0 and 14.6 Hz, 1H, βCH), 3.29 (dd, *J* = 5.8 and 14.6 Hz, 1H, βCH), 3.70 (q, *J* = 7.2 Hz, 1H, CH), 3.71 (s, 3H, OCH_3), 3.96 (s, 3H, OCH_3 Npx), 4.71−4.78 (m, 1H, αCH), 5.83 (s, 1H, βCH), 5.98 (d, *J* = 7.2 Hz, 1H, NH), 6.53 (s, 1H, βCH), 6.58 (s, 1H, 2-CH Trp), 7.03 (dt, *J* = 0.8 and 7.2 Hz, 1H, Ar H Trp), 7.13 (t, *J* = 2.4 Hz, 1H, Ar H Npx), 7.16−7.17 (m, 1H, Ar H Trp), 7.18 (dd, *J* = 2.8 and 8.8 Hz, 1H, Ar H Npx), 7.25−7.28 (m, 1H, Ar H Trp), 7.27−7.29 (m, 1H, Ar H Npx), 7.49 (d, *J* = 8.0 Hz, 1H, Ar H Trp), 7.54 (d, *J* = 1.2 Hz, 1H, Ar H Npx), 7.63−7.67 (m, 3H, 2 × Ar H Npx and NH), 8.02 (s, 1H, NH); ^{13}C NMR (100.6 MHz, $CDCl_3$, δ): 18.12 (CH_3), 27.32 (βCH_2), 47.08 (CH), 52.77 (OCH_3), 54.25 (αCH), 55.35 (OCH_3 Npx), 105.57 (CH Npx), 109.20 (βCH_2), 109.74 (3-C Trp), 111.07 (CH Trp), 118.71 (CH Trp), 119.03 (CH Npx), 119.78 (CH Trp), 122.28 (CH Trp), 122.92 (2-CH Trp), 126.18 (CH Npx), 126.30 (CH Npx), 127.03 (3a-C Trp), 127.59 (CH Npx), 129.01 (C Npx), 129.41 (CH Npx), 130.61 (αC), 133.78 (C Npx), 135.43 (2-C Npx), 136.07 (7a-C Trp), 157.77 (6-C Npx), 163.82 (C═O ΔAla), 169.99 (C═O Trp), 174.81 (C═O Npx); HRMS (ESI) *m/z*: $[M + H]^+$ calcd for $C_{29}H_{30}N_3O_5^+$, 500.2180; found, 500.2178.

Synthesis of the (*S*)-(+)-Naproxen *N*-Capped *C*-Deprotected Dehydropeptides (7a−c). The (*S*)-(+)-naproxen-dehydrodipeptide was dissolved in 1,4-dioxane (until 10 mL mmol^{-1}) and NaOH (1 M) (1.5 equiv). The reaction was followed by TLC until no starting material was detected. The organic solvent was removed under reduced pressure, and the reaction mixture was acidified to pH 3 with $KHSO_4$ (1 M). The solid formed was filtered, affording compounds **7a−c**.

*Npx-L-Trp-Z-ΔPhe-OH (**7a**).* Npx-L-Trp-Z-ΔPhe-OMe (**6a**) (0.14 g, 0.25 mmol) gave compound **7a** as a white solid (0.13 g, 93%); mp: 199.0−200.0 °C; ^{1}H NMR (400 MHz, DMSO-d_6, δ): 1.23 (d, *J* = 7.2 Hz, 3H, CH_3), 2.99 (dd, *J* = 9.6 and 14.4 Hz, 1H, βCH), 3.24 (dd, *J* = 4.4. and 14.4 Hz, 1H, βCH), 3.79 (q, *J* = 7.2 Hz, 1H, CH), 3.83 (s, 3H, OCH_3), 4.76−4.81 (m, 1H, αCH), 6.99 (dt, *J* = 0.8 and 7.2 Hz, 1H, Ar H), 7.05−7.15 (m, 5H, Ar H), 7.20−7.25 (m, 3H, Ar H and βCH), 7.34−7.40 (m, 2H, Ar H), 7.49 (d, *J* = 6.4 Hz, 2H, Ar H), 7.64−7.70 (m, 4H, Ar H), 8.25 (d, *J* = 8.4 Hz, 1H, NH Trp), 9.65 (s, 1H, NH ΔPhe), 10.83 (d, *J* = 1.6 Hz, 1H,1-NH Trp), 12.63 (brs, 1H, CO_2H); ^{13}C NMR (100.6 MHz, DMSO-d_6, δ): 18.84 (CH_3), 27.65 (βCH_2), 44.60 (CH), 53.32 (αCH), 55.10 (OCH_3), 105.61 (CH), 110.07 (C), 111.24 (CH), 118.16 (CH), 118.36 (CH), 118.56 (CH), 120.82 (CH), 123.76 (CH), 125.33 (CH), 126.40 (CH), 126.48 (C), 126.64 (CH), 127.41 (C), 128.28 (CH), 128.31 (C), 128.89 (CH), 129.05 (CH), 129.82 (CH), 131.56 (βCH), 133.02 (C), 133.59 (C), 136.06 (C), 137.22 (C), 156.88 (C), 166.27 (C═O ΔPhe), 171.25 (C═O Trp), 173.31 (C═O Npx); HRMS (ESI) *m/z*: $[M + H]^+$ calcd for $C_{34}H_{32}N_3O_5^+$ 562.23365; found, 562.23306; $[M + Na]^+$ calcd for $C_{34}H_{31}N_3NaO_5^+$, 584.2156; found, 584.2150.

*Npx-L-Trp-Z-ΔAbu-OH (**7b**).* Npx-L-Trp-Z-ΔAbu-OMe (**6b**) (0.37 g, 0.72 mmol) gave compound **7b** as a cream solid (0.29 g, 81%); mp: 187.0−190.0 °C; ^{1}H NMR (400 MHz, DMSO-d_6, δ): 1.22 (d, *J* = 6.8 Hz, 3H, CH_3 Npx), 1.43 (d, *J* = 6.8 Hz, 3H, CH_3 ΔAbu), 2.98 (dd, *J* = 9.6 and 14.8 Hz, 1H, βCH), 3.19 (dd, *J* = 5.2 and 14.8 Hz, 1H, βCH), 3.78 (q, *J* = 6.8 Hz, 1H, CH), 3.84 (s, 3H, OCH_3), 4.70−4.75 (m, 1H, αCH), 6.49 (q, *J* = 6.8 Hz, 1H, βCH), 6.98 (dt, *J* = 0.6 and 7.3 Hz, 1H, CH-5 Trp), 7.06 (dt, *J* = 1.0 and 7.5 Hz, 1H, CH-6 Trp), 7.10 (dd, *J* = 2.8 and 8.8 Hz, 1H, CH-7 Npx), 7.19 (d, *J* = 2.4 Hz, 1H, CH-2 Trp), 7.23 (d, *J* = 2.4 Hz, 1H, CH-5 Npx), 7.32 (d, *J* = 8.0 Hz, 1H, CH-7 Trp), 7.37 (dd, *J* = 1.6 and 8.4 Hz, 1H, CH-6 Npx), 7.64−7.72 (m, 4H, CH-4 Trp, CH-1 Npx, CH-4 Npx, CH-8 Npx), 8.21 (d, *J* = 8.4 Hz, 1H, αNH Trp), 9.14 (s, 1H, NH ΔAbu), 10.81 (d, *J* = 1.6 Hz, 1H, NH-1 Trp), 12.42 (brs, 1H, CO_2H); ^{13}C NMR (100.6 MHz, DMSO-d_6, δ): 13.46 (CH_3 ΔAbu), 18.49 (CH_3 Npx), 28.09 (βCH_2), 44.54

DOI: 10.1021/acs.biomac.5b01006
Biomacromolecules 2015, 16, 3562−3573

Scheme 1. Synthesis of *N*-Capped Naproxen Dehydrodipeptides 7a−c[a]

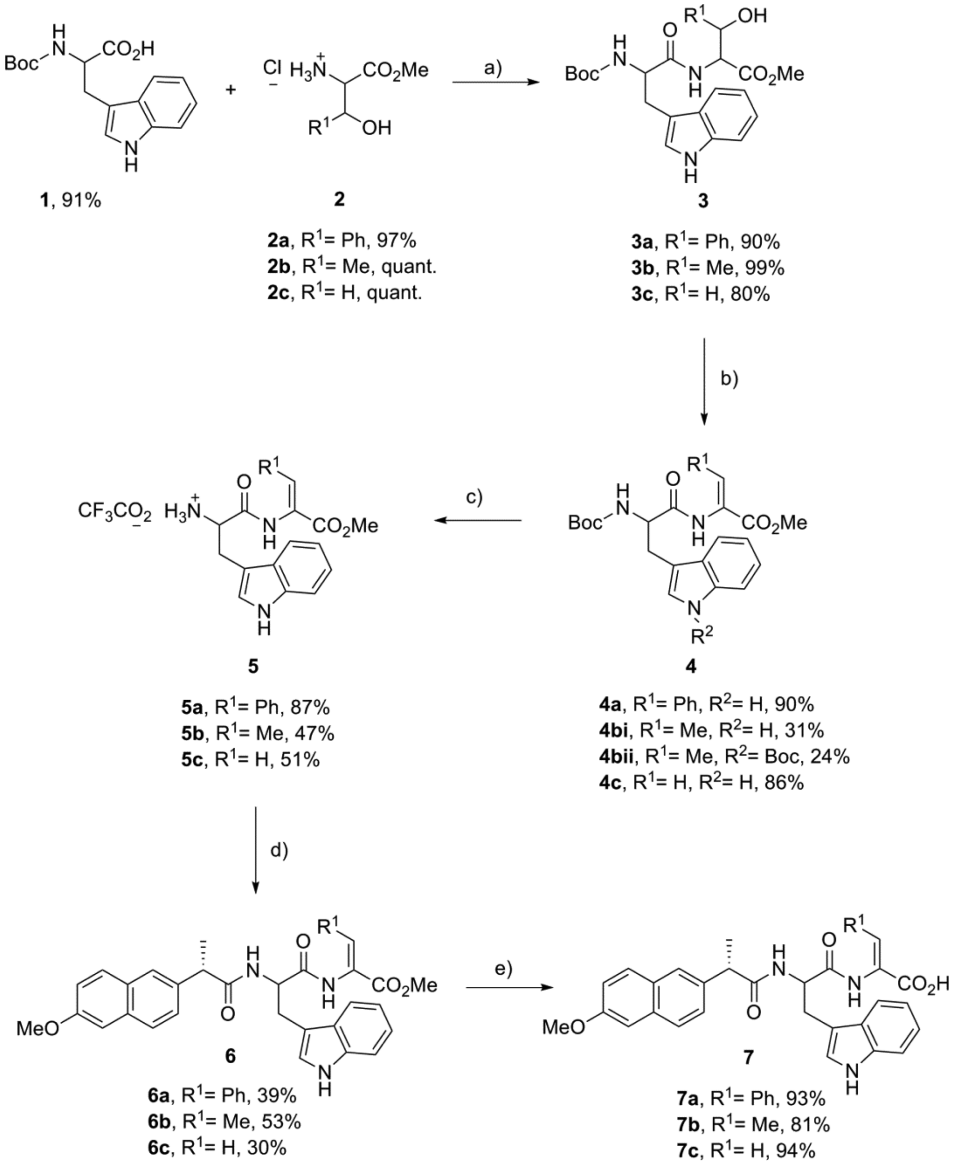

[a](a) DCC, HOBt, Et_3N, ACN, rt, 18 h; (b) (1) Boc_2O, DMAP, dry ACN, rt, (2) TMG; (c) TFA, rt; (d) (*S*)-(+)-naproxen chloride, Et_3N, DCM, rt, 18 h; (e) (1) NaOH (1 M), 1,4-dioxane, rt, (2) $KHSO_4$ (1 M).

(CH), 53.26 (αCH), 55.10 (OCH_3 Npx), 105.62 (CH-5 Npx), 110.05 (C-3 Trp), 111.20 (CH-7 Trp), 118.14 (CH-5 Trp), 118.41 (CH-7 Npx), 118.57 (CH-4 Trp), 120.79 (CH-6 Trp), 123.69 (CH-2 Trp), 125.27 (CH-1 Npx), 126.41 (CH-4 Npx), 126.59 (CH-3 Npx), 127.45 (C-3a Trp), 128.07 (C-8a Npx), 128.31 (αC), 129.04 (CH-8 Npx), 132.13 (βCH), 133.03 (C-4a Npx), 136.02 (C-7a Trp), 137.15 (C-2 Npx), 156.90 (C-6 Npx), 165.41 (C═O ΔAbu), 170.26 (C═O Trp), 173.16 (C═O Npx); HRMS (ESI) *m*/*z*: $[M + H]^+$ calcd for $C_{29}H_{30}N_3O_5^+$, 500.2180; found, 500.2178.

*Npx-L-Trp-ΔAla-OH (**7c**).* Npx-L-Trp-ΔAla-OMe (**6c**) (90 mg, 0.20 mmol) gave compound **7c** as a white foam (90.8 mg, 94%); mp: 100.0−105.0 °C; ^{1}H NMR (400 MHz, DMSO-d_6, δ): 1.25 (d, *J* = 7.2 Hz, 3H, CH_3), 3.01 (dd, *J* = 9.2 and 14.8 Hz, 1H, βCH), 3.21 (dd, *J* = 4.8 and 154.8 Hz, 1H, βCH), 3.79 (q, *J* = 7.2 Hz, 1H, CH), 3.84 (s, 3H, OCH_3), 4.70−4.75 (m, 1H, αCH), 5.66 (s, 1H, βCH), 6.25 (s, 1H, βCH), 6.97 (dt, *J* = 0.8 and 6.8 Hz, 1H, Ar H Trp), 7.06 (dt, *J* = 1.2 and 8.0 Hz, 1H, Ar H Trp), 7.09−7.15 (m, 2H, Ar H), 7.26 (dd, *J* = 2.4 and 16.8 Hz, 1H, Ar H), 7.32−7.41 (m, 2H, Ar H), 7.59−7.71 (m, 4H, Ar H), 8.42 (d, *J* = 8.0 Hz, 1H, NH Trp), 9.06 (s, 1H, NH ΔAla), 9.82 (s, 1H, 1-NH Trp), 12.58 (brs, 1H, CO_2H); ^{13}C NMR (100.6 MHz, DMSO-d_6, δ): 18.51 (CH_3), 26.95 (βCH_2), 44.69 (CH), 54.16 (αCH), 55.12 (OCH_3), 105.65 (CH), 107.66 (βCH_2), 109.99 (C), 111.29 (CH), 118.26 (CH), 118.40 (CH), 118.68 (CH), 120.87 (CH), 123.60 (CH), 125.24 (CH), 126.53 (CH), 126.83 (CH), 127.31 (C), 128.34 (C), 129.07 (CH), 132.63 (αC), 133.07 (C), 136.05 (C), 136.86 (C), 156.95 (C), 164.72 (CO_2H), 170.89 (C═O Trp), 173.75 (C═O Npx); HRMS (ESI) *m*/*z*: $[M + H]^+$ calcd for $C_{28}H_{28}N_3O_5^+$ 486.20235; found, 486.20270; $[M + Na]^+$ calcd for $C_{28}H_{27}N_3NaO_5^+$, 508.1843; found, 508.1851.

Compound **8** [methyl 3-amino-6-(benzo[*d*]thiazol-2-ylamino)-thieno[3,2-*b*]pyridine-2-carboxylate] was previously synthesized.[30]

RESULTS AND DISCUSSION

Synthesis. In this work, we investigate the effect of different *C*-terminal dehydroamino acids (ΔAbu, ΔPhe, and ΔAla) on the gelation of dehydrodipeptides (**7a−c**) containing a naproxen-capped *N*-terminal Trp residue (Scheme 1). For the synthesis of dehydrodipeptides (**7a−c**), a block synthesis strategy in solution was adopted (Scheme 1). Orthogonally

DOI: 10.1021/acs.biomac.5b01006
Biomacromolecules 2015, 16, 3562−3573

protected dipeptides (**3a−c**), containing a *N*-*tert*-butyloxycarbonyl (*N*-Boc) protected Trp residue and ester protected *C*-terminal *β*-hydroxyamino acids, were synthesized in good to excellent yields by coupling Boc-L-Trp-OH (**1**) to the amino acids methyl esters **2a−c** using the standard *N*,*N*′-dicyclohexylcarbodiimide (DCC)/1-hydroxybenzotriazole (HOBt) procedure. Reacting dipeptides **3a** and **3c** with one equivalent of di-*tert*-butyl dicarbonate (Boc_2O) in the presence of 4-dimethylaminopyridine (DMAP), followed by *N*,*N*,*N*′,*N*′-tetramethylguadinine (TMG), afforded dehydropeptides **4a** and **4c** in good yields (Scheme 1). Under the same conditions, peptide **3b** gave a mixture of Boc-L-Trp-*Z*-ΔAbu-OMe (**4bi**) and Boc-L-Trp(*N*-Boc)-*Z*-ΔAbu-OMe (**4bii**) in 54% aggregate yield. Attempts to improve the yield of **4b** proved unsuccessful: use of Boc_2O in excess (4.5 mol equiv) generated a complex mixture of dehydration products that could not be resolved by chromatography. Under these conditions (excess Boc_2O), peptide **3c** also afforded a complex mixture of dehydration products. Dehydropeptides **4a−c** were obtained with stereoselectivity toward the *Z*-isomer in agreement with previous reports from our research group.[38] Orthogonal *N*-deprotection of dehydropeptides **4a−c** with trifluoroacetic acid (TFA) allowed *N*-capping the *C*-protected dehydropeptides **5a−c** with (*S*)-(+)-naproxen by treatment with (*S*)-(+)-naproxen chloride (Npx-Cl) in the presence of triethylamine (Et_3N). Naproxen amides are prone to racemization under the dehydration conditions employed in this work. Capping the dehydrated peptides minimizes the extent of racemization of the stereogenic center in the naproxen moiety. Naproxen *N*-capped *C*-deprotected dehydropeptides **7a−c** were obtained in good to excellent yields by saponification with diluted aqueous NaOH (Scheme 1). ^{1}H NMR spectra of compounds **7a−c** are included in the Supporting Information (Figures S2−S4).

Preparation of Hydrogels. With dehydrodipeptides **7a−c** in hand, different methodologies were evaluated for obtaining molecular hydrogels via self-assembly in solution. Hydrogelators **7a−c** revealed very low solubility in buffer solutions (pH 6−8) both at rt and at 60 °C. Nonetheless, dehydrodipeptides **7a−c** could be dissolved in water at 60 °C upon adjustment of suspensions to pH ≈ 10−11. Gel formation was attained for peptides **7a** and **7b** by slow pH dropping triggered by hydrolysis of added D-glucono-*δ*-lactone (GdL). For peptide **7c**, hydrogelation could not be attained by addition of GdL; suspensions and precipitates were obtained depending on hydrogelator concentration, GdL/NaOH ratio, and final pH of the test solutions. Dehydrodipeptide **7c** gelled through (fast) pH dropping by addition of diluted hydrochloric acid (1 M). In general, GdL is preferred for triggering gelation owing to formation of more uniform gels.[39] A comprehensive study, aiming at optimizing the experimental conditions for gelation, was carried out for hydrogelators **7a−c**. The results of this study are best understood as "phase diagrams", showing the dependence of the final pH of test solutions on peptide concentration or GdL/NaOH ratio (for **7a** and **7b**) and HCl/NaOH (for **7c**) employed for gelation and the macroscopic appearance (gel/precipitate/suspension/solution) of the test solution. Phase diagrams for hydrogelators **7a−c** are included in the Supporting Information (Figures S5−S7).

Table 1 summarizes the optimized conditions for gelation of peptides **7a−c**. For additional information and images of the gels, please see the Supporting Information (Figures S8−S10).

The critical gelation concentration (CGC) for peptides **7a−c** (Table 1) seems to follow a general correlation with peptide hydrophobicity; hydrogelators exhibiting higher hydrophobicity (**7a** > **7b** > **7c**) display lower CGC (at a similar pH).[27c] In general, the pH at which gel is formed is highly dependent on the molecular structure of the hydrogelator and seems to correlate with the apparent pK_a of the peptide.[27b] Hydrogelators **7a** and **7b** present gelation pH values significantly lower than similar dehydropeptides containing a Phe replacing the Trp residue (Npx-L-Phe-*Z*-ΔPhe-OH, gelation at pH 8 and Npx-L-Phe-*Z*-ΔAbu−OH, gelation at pH 6),[22] presumably owing to higher hydrophilicity of the indole moiety. Moreover, peptide **7b** also gels at lower pH than **7a**, presumably owing to higher hydrophobicity. This trend is not followed by **7c**, probably owing to the fast pH drop that results from the addition of hydrochloric acid. The slower kinetics of pH dropping attained with GdL is likely to allow the molecules to organize and self-assemble without precipitating, while the fast drop in pH produced by the addition of hydrochloric acid is prone to lead to precipitation.

Table 1. Optimized Conditions for Gelation of Peptides 7a−c

	critical gelation concentration (CGC)		GdL concentration	GdL/NaOH ratio	
	[wt %]	[mM]	[wt %]	[wt %/%v/v]	pH
7a	0.40	7.05	0.58	0.17	4.61
	0.40	7.12	0.34	0.24	4.73
	0.41	7.30	0.34	0.14	5.68
7b	0.66	13.21	0.83	0.42	3.82
	0.61	12.21	0.56	0.33	3.88
	0.60	12.01	0.34	0.14	5.81
	0.49	9.81	0.37	0.15	4.75
	0.41	8.21	0.49	0.20	4.23
7c	0.67	13.80			5.75
	0.64	13.18			5.76
	0.60	12.36			6.86

Interestingly, it was observed that when a gel is broken by an external mechanical force (e.g., in rheological measurements), the pH of the broken gel/suspension is about 0.5−3.0 pH units higher than the intact gel (same concentration of hydrogelator and ratio GdL/NaOH). This indicates that the network that constitutes the gel influences the pH.[25,39]

UV−vis Absorption Spectroscopy and Circular Dichroism (CD). The absorption spectra of compounds **7a−c** are very similar (Figures S11B, S12B, and S13B), typical of naphthalene and substituted naphthalene compounds.[27b] The spectra are dominated by the absorption of the naproxen moiety: a weak band between 310 and 340 nm (observed only in some hydrogelators/gels), a medium band at 260−290 nm, and an intense signal between 210 and 240 nm. The absorption band between 260 and 290 nm is attributed to the naphthalene $\pi-\pi^*$ short axis polarized transition,[27b,40] and much of the band around 225 nm and the band above 300 nm are attributed to naphthalene $\pi-\pi^*$ long axis polarized transitions.[27b,40] The peptide transitions, between 210 and 230 (n-π^* transitions) and 180−200 nm ($\pi-\pi^*$ transitions),[41] are usually weaker than those assigned to the naphthalene moiety. The self-assembly of peptides **7a−c** was studied by CD spectroscopy (Figure 1).

To avoid scattering effects (important in turbid gels), CD measurements were carried out on diluted peptide solutions. Peptides **7a−c** display similar CD spectra suggesting a similar arrangement of the individual molecules into a dense network

DOI: 10.1021/acs.biomac.5b01006
Biomacromolecules 2015, 16, 3562−3573

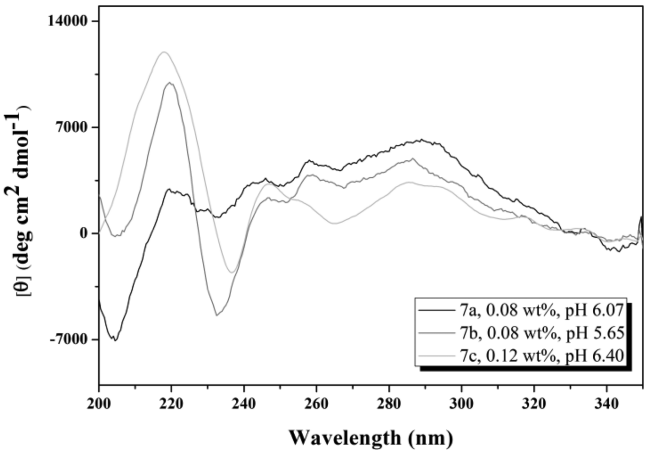

Figure 1. CD spectra of diluted solutions of dehydrodipeptides **7a**−**c**.

of long fibers. This was confirmed by TEM measurements using the same solutions used for the CD study (Figure 5). A broad positive Cotton effect, assigned to the $\pi-\pi^*$ short axis polarized transitions of naphthalene, is observed around 287 nm.[27b,40] The absorbance band at λ = 225 nm results in exciton couplets, evidenced by the positive and negative Cotton effects at 219 and 233 nm, with zero at the absorbance maximum.[41,42] The sign of the Cotton effect associated with each exciton couplet indicates the helicity of the chiral arrangement: peptides **7a**−**c** exhibit left-handed helical naphthalene arrangements.[42] This effect indicates that the naproxen groups are highly organized through chiral stacking. The weaker exciton coupling observed around 225 nm for peptide **7a**, comparing to **7b** and **7c**, indicates lower chiral ordering of the aggregates of peptide **7a**. The higher intensity of the Cotton effect observed for **7a** around 287 nm suggests stronger intermolecular interactions in the peptide aggregates compared to **7b** and **7c**. Interference between the CD signal of the naphthalene moieties and the signals of the Phe and Trp residues, around 225 and 280 nm, cannot be ruled out.[3,19,41] The Trp indole side chain CD transitions, usually observed at 250−300 nm, 225−235 nm, and 190−210 nm,[41] are likely masked by the signals of the naphthalene and amide groups. Very similar CD spectra were obtained for solutions of dehydrodipeptide **7c**, adjusted either with diluted hydrochloric acid or GdL (same concentration and pH) (Figure S13A), suggesting an identical arrangement of the hydrogelator molecules into fibers, as confirmed by TEM studies (Figure 5D,F).

Hydrolysed GdL (gluconic acid), although CD silent above 200 nm, is active below 200 nm (Figure S1) potentially interfering with the CD signal of the peptide $\pi-\pi^*$ transition (UV absorption at 180−200 nm). The peptide n−π^* transition (UV absorption at 210−230 nm) is likely masked by the Cotton effect of the naphthalene moiety. In this work, we were not able establish the arrangement of the peptide backbone (secondary structure) of the dehydrodipeptide molecules in the fibers.[42]

The CD spectra of gels of dehydrodipeptides **7a** (Figure S11A) and **7b** (Figure S12A) display features identical to the solution spectra, suggesting a similar assembly of the peptide molecules in the fibers. Gels could not be obtained for peptide **7c** by the GdL methodology. Turbid gels were obtained by pH adjustment with dilute hydrochloric acid. This indicates that the presence of salts and the gelation kinetics, in addition to pH, play an important role in the self-assembly process.[43]

Fluorescence Studies. The influence of pH and hydrogelator concentration on the self-assembly behavior of peptide **7a** was investigated taking advantage of the intrinsic fluorophore naproxen (Figure 2). The fluorescence spectrum

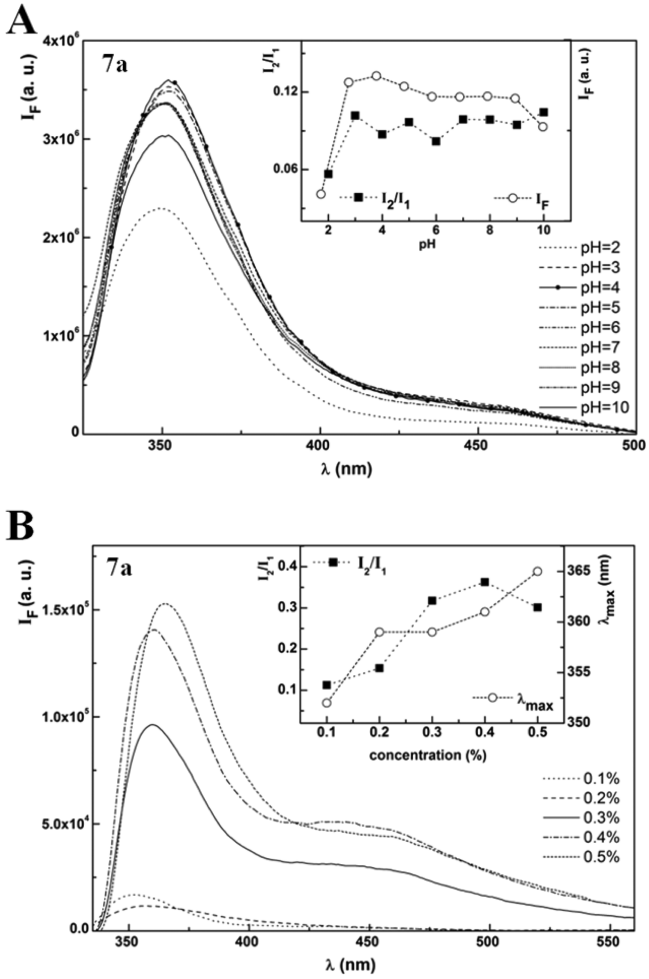

Figure 2. (A) Fluorescence spectra (λ_{exc}= 290 nm) of dehydrodipeptide **7a** (A) at 2 × 10^{-6} M in the pH range 2−10. Inset: pH dependence of the maximum fluorescence intensity (I_F) and of the intensity ratio I_2/I_1 of the naproxen aggregate band (I_2) and the naproxen monomer band (I_1). (B) Fluorescence spectra (λ_{exc} = 290 nm) of dehydrodipeptide **7a** in the concentration range 0.1−0.5 wt %, pH 6 (adjusted with GdL). Inset: concentration dependence of the wavelength of maximum emission of the naproxen monomer band (λ_{max}) and of the intensity ratio I_2/I_1 of the naproxen aggregate (I_2) and monomer band (I_1).

of peptide **7a** shows a main band at 353 nm (λ_{exc} = 290 nm), as reported for naproxen in methanol and water,[40] and a second fluorescence band with maximum emission near 440 nm. At the excitation wavelength (λ_{exc} = 290 nm) both the naproxen moiety and the indole group of Trp are directly excited (ε = 1336 M^{-1} cm^{-1} and 1778 M^{-1} cm^{-1} for naproxen[40] and indole,[44] respectively, at 290 nm in aqueous media) displaying also similar fluorescence emission spectra (λ_{max} = 353 and 355 nm for naproxen and Trp, respectively, in water at pH 7).[45] The fluorescence spectrum is likely to be dominated by the naproxen emission thanks to its higher fluorescence quantum yield (Φ_F= 0.41[40] and 0.20[44] for naproxen and indole, respectively, in aqueous medium) (Figure 2). The low intensity broad band at 440 nm, pH- and concentration-dependent, was

DOI: 10.1021/acs.biomac.5b01006
Biomacromolecules 2015, 16, 3562−3573

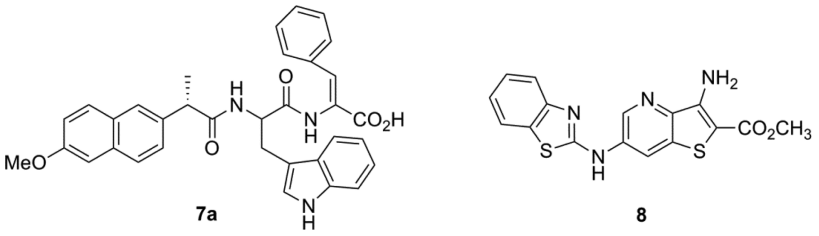

Figure 3. Structures of carrier dehydrodipeptide **7a** (Npx-L-Trp-*Z*-ΔPhe-OH) and of antitumor compound **8** (methyl 3-amino-6-(benzo[*d*]thiazol-2-ylamino)thieno[3,2-*b*]pyridine-2-carboxylate).

assigned to the formation of emissive aggregates, as reported by us for hydrogelators containing naproxen and aromatic moieties.[22] The pH dependence of the fluorescence emission at 355 nm is relatively weak (Figure 2A), attaining stabilization at pH 6−9. The ratio I_2/I_1 of the intensity of the aggregate band (F_{440}, I_2) and naproxen monomer band (F_{353}, I_1) reaches a maximum at pH ≈ 3, near the pK_a value of the peptide terminal carboxylic acid (pK_a ≈ 3),[45] stabilizing thereafter.

The concentration dependence of the fluorescence emission of peptide **7a** shows that the ratio of intensities of the aggregate and monomer bands, I_2/I_1 (inset in Figure 2B), reaches a maximum at 0.4 wt %, stabilizing thereafter. A clear red shift of the naproxen maximum emission wavelength is also observed above 0.4 wt %. Thus, 0.4 wt % can be interpreted as the CGC of the hydrogelator. The aggregation of the peptide molecules seems to be driven by $\pi-\pi$ stacking intermolecular interactions.[18a,46] This value (0.4 wt %) agrees well with the CGC value determined experimentally (Table 1).

Npx-L-Trp-*Z*-ΔPhe-OH (7a) Gel as Nanocarrier for Drugs. The ability of hydrogel **7a** (Figure 3) to act as nanocarrier for incorporated (noncovalently bound) low molecular weight drugs was investigated using the potential antitumor thieno[3,2-*b*]pyridine derivative **8** (Figure 3). This compound is a potent growth inhibitor of several human cancer cell lines, MCF-7 (breast adenocarcinoma), A375-C5 (melanoma), and NCI-H460 (nonsmall cell lung cancer), being remarkably active against the melanoma cell line.[30] Compound **8** also exhibits also low affinity for the multidrug resistance protein MDR1[47] that promotes drug resistance in cells. Compound **8** displays ideal properties for use as model compound to study the ability of gel **7a** to act as nanocarrier for drugs: compound **8** is fluorescent in several polar and nonpolar solvents but not in aqueous media; its fluorescence emission is characterized by a large nonstructured band (maximum wavelength between 450 and 500 nm) displaying a red shift with increasing solvent polarity.[47]

The spectral overlap between hydrogel emission (energy donor) and compound **8** absorption (energy acceptor) indicates the possibility of resonance energy transfer (FRET) between hydrogel **7a** and compound **8** as long as the distance donor−acceptor is under 100 Å (Figure 4A). Energy transfer from excited hydrogel groups to the antitumor compound can be observed by exciting the hydrogel (λ_{exc} = 290 nm) (Figure 4B).

Although compound **8** is also directly excited at 290 nm (Figure 4A), the occurrence of FRET is made clear by the decrease of intensity of the Npx/Trp emission band and a significant enhancement of the emission of compound **8** (λ_{max} ≈ 450 nm) incorporated in the gel. A strong emission band is observed at λ_{em} = 445 nm when compound **8** (incorporated in the gel) is selectively excited (λ_{exc} = 360 nm), indicating that

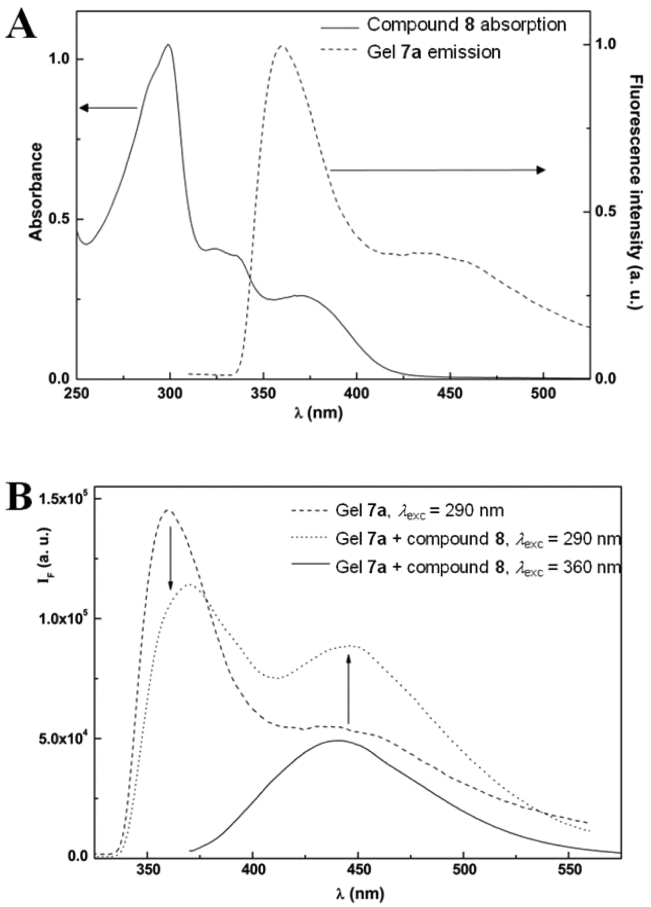

Figure 4. (A) Spectral overlap between compound **8** absorption and hydrogel **7a** emission (normalized spectra). (B) Fluorescence spectra of hydrogel **7a** at 0.4 wt % (λ_{exc} = 290 nm) and hydrogel **7a** with compound **8** (3×10^{-6} M) incorporated, exciting the hydrogel (λ_{exc} = 290 nm) and exciting selectively compound **8** (λ_{exc} = 360 nm).

the drug is not located in the bulk water solvent, where it is not fluorescent, but instead is located in a hydrophobic microenvironment with a polarity similar to cyclohexane, presumably near (inside) the hydrogel fibers (Figure 4B).[47] The fluorescence quantum yield of the hydrogel (donor), Φ_F = 0.04, was determined using the standard method (eq 5). A FRET efficiency, Φ_{RET}, of 21% was calculated (see Materials and Methods section) with a corresponding donor−acceptor distance of 2.3 nm. This distance is very similar to that obtained for the binding of this drug by the native form of BSA (pH 7).[47]

Transmission Electron Microscopy. The micro/nanostructure of the three-dimensional network of the hydrogels was investigated by TEM. All peptides form extended fibrous networks (Figure 5). Peptide **7a** produced a heterogeneous

DOI: 10.1021/acs.biomac.5b01006
Biomacromolecules 2015, 16, 3562−3573

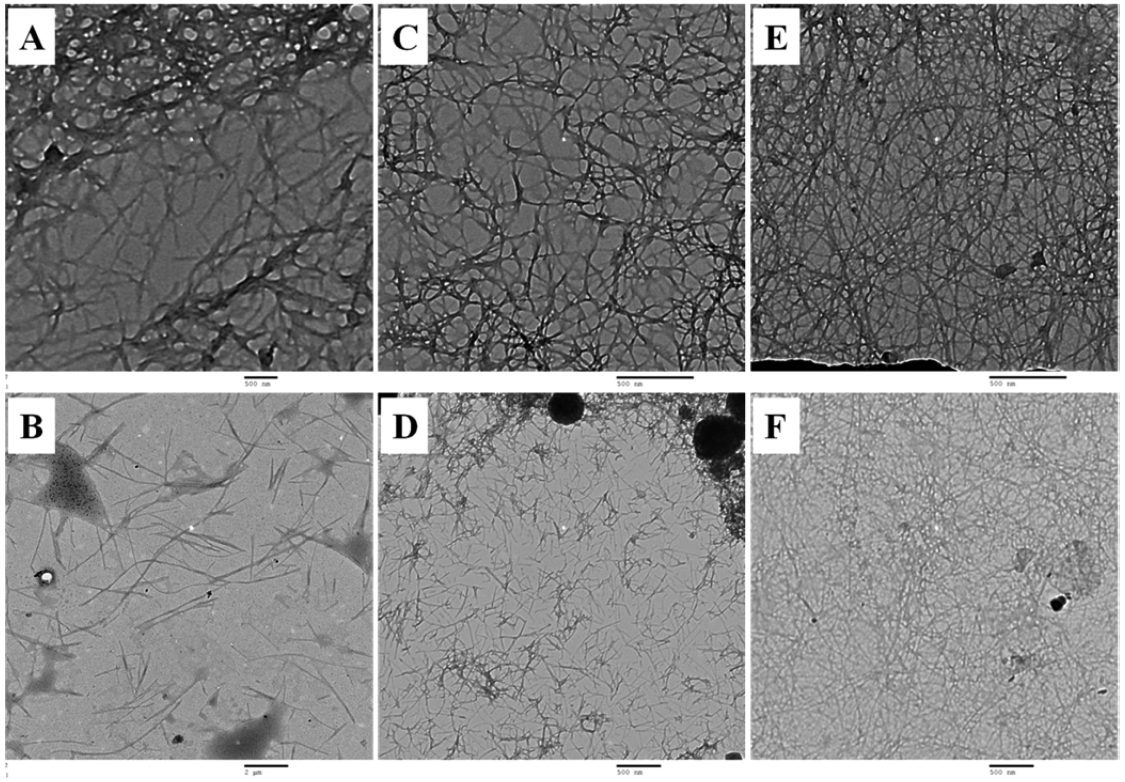

Figure 5. TEM images of dehydrodipeptides **7a–c** obtained from stained and dried samples of (A) **7a**, 0.08 wt %, pH 6.07 (GdL), scale bar 500 nm; (B) **7a**, 0.08 wt %, pH 6.07 (GdL), scale bar 2 μm; (C) **7b**, 0.08 wt %, pH 5.65 (GdL), scale bar 500 nm; (D) **7b**, 0.08 wt %, pH 5.65 (GdL), scale bar 500 nm; (E) **7c**, 0.12 wt %, pH 6.26 (HCl), scale bar 500 nm; (F) **7c**, 0.12 wt %, pH 6.40 (GdL), scale bar 500 nm.

Table 2. Rheological Properties of Hydrogels of Dehydrodipeptides 7a–c

	dehydrodipeptide concentration			GdL concentration			strain[b]	stress[b]	Young's modulus[c]	shear modulus[e]
	[wt %]	[mM]	pH[a]	[wt %]	[mM]	[equiv]	[%]	[Pa]	[Pa]	[Pa]
7a	0.41	7.30	7.83	0.34	19.09	2.62	30.2	801.3	3266.6 ± 7.7	1088.9
			6.91	0.40	22.45	3.19	8.2	4319.7	56117.9 ± 120.1	18706.0
			4.61	0.60	33.68	4.79	2.0	5246.6	310604.9 ± 4898.5	103535.0
7b	0.39	7.81	3.88	0.98	55.01	7.04	11.6	549.0	796.3 ± 167.7	265.4
	0.40	8.01	6.74	0.43	24.14	3.01	12.1	1854.8	5736.4 ± 90.6	1912.1
							12.4[d]	383.3[d]	1678.3 ± 34.4[d]	559.4
	0.50	10.01	6.94	0.40	22.45	2.24	14.3	531.1	2966.0 ± 11.7	988.7
							14.6[d]	191.4[d]	1219.7 ± 9.2[d]	406.6
	0.59	11.81	7.06	0.42	23.58	2.00	10.8	982.5	3611.4 ± 89.3	1203.8
7c	0.58	11.95	5.75				14.4	2146.5	4127.9 ± 61.0	1376.0

[a]Measured after breaking in the remaining gel. [b]Values taken at the breaking point. [c]Determined from the slope of the linear regime of the stress–strain response curve. [d]Values for the recovered gels after shear breaking. [e]Determined from Young's moduli ($G = E/3$).[31]

fibrous structure with variable density (Figure 5A). In the most concentrated areas, the fibers display thicknesses ranging from 44–73 nm. In the less dense zones, thicker fibers are found, with diameters between 98 and 260 nm and lengths between 2 and 11 μm (Figure 5B). Peptide **7b** also showed a heterogeneous dense 3D network of fibers (Figure 5C) with diameters between 15 and 24 nm. In the areas of lower density, the fibers are shorter, with lengths between 150 and 400 nm, but similar thickness (Figure 5D). Hydrogels of compound **7c**, formed by pH decrease by addition of either HCl or GdL, presented very similar fiber networks (Figure 5E,F), which were long and homogeneous thin fibers, with diameter between 12 and 19 nm, forming a network much denser (more connectivity between the fibers) than the ones formed by peptides **7a** and **7b**. The fibers are also more homogeneous than those formed by peptides **7a** and **7b**.

Rheology. *In situ* gel setting in the rotational rheometer was hampered by slow gelation kinetics of peptides **7a–c** and their sensitivity to external forces during the gelation process. The large strains needed to record torque levels above the sensitivity limit of the rheometer were in fact breaking up the forming gels. The time evolution of the storage (G') and loss (G'') moduli could not be measured. Penetration tests on equilibrated gels were used instead to determine the elasticity of the peptide gels **7a–c**.

Hydrogels of peptide **7a** display higher elasticity (measured by Young's moduli) at lower pH (measured for the broken gels). Gel pH seems to be determined by the amount of GdL

DOI: 10.1021/acs.biomac.5b01006
Biomacromolecules 2015, 16, 3562–3573

used for gelation (Figure S14A, Table 2). Hydrogels of compound **7a** are brittle, that is, they fracture (undergo irreversible break with water expulsion) right after the linear regime of the stress−strain curves (Figure S14A). Moreover, gels formed at lower pH values revealed more brittle, that is, they fracture at lower strains (Table 2). In contrast, gels of peptides **7b** and **7c** revealed strain hardening responses after the linear regime, followed by fracture at strains between 11 and 14% (Figure S14B,C). This mechanical behavior under large deformation is consistent with the stranded morphology of the gels revealed by TEM (Figure 5).[48] For peptide **7b**, the pH after gel fracturing by mechanical testing correlates with the number of added molar equivalents of GdL (Table 2). The dependence of the elasticity of gels of peptide **7b** on gelator and GdL concentration (Figure S14D) suggests that both peptide and GdL concentration influence hydrogel elasticity.[25] For peptide **7b** at 0.4 wt %, an increase in GdL concentration from around 0.4 to 1 wt %, which results in a decrease of the final pH of the gels from around 7 to 4, leads to a significant decrease in gel elasticity (Figure S14B,D). The amount of added GdL influences the kinetics of gelation and the final pH of the gel.[25,27b,49] While the final pH of the gel has been reported as a determining factor for gel elasticity,[50] the kinetics of gelation influences some of the mechanical properties of the gels, but not the storage modulus (which relates to Young's modulus) for this kind of hydrogel.[25,27b] Gels of peptides **7b** and **7c**, despite displaying overall lower elasticity than gels of peptide **7a**, exhibit structural healing properties, that is, structural recovery after fracture with buildup of a new gel. The gels of peptide **7b** at 0.40 and 0.50 wt % recovered a few days after mechanical testing with fracture. The recovered gels revealed only a small change of the strain at fracture, but a significant decrease of elasticity (Young's moduli), about five times for the 0.4 wt % gel and around two times for the 0.5 wt % gel, showing only partial recovery (Figure S14B). The (similar) elasticity, strain hardening behavior, and recovery properties exhibited by the gels of peptides **7b** and **7c** are likely related to the nano/microarchitecture of their fiber networks: high density networks made of fibers with similar thickness (Figure 5).

Young's moduli E can be converted to the shear modulus G for the purpose of comparing the elasticity of gels **7a−c** with other peptide gels characterized by rotational rheometry (time evolution of the storage G' and loss G'' moduli). Assuming that gels are incompressible, G is of the same order of magnitude as G', $G' \approx G = E/3$.[31] Gels of peptides **7a−c** display shear moduli G in the range 10^2-10^5 Pa (Table 2). These values are comparable to the elasticity reported for gels of other *N*-protected dipeptides, usually characterized by G' values in the range of 10^2-10^4 Pa[27,51] and less often G' values around 10^5 Pa.[3,25]

CONCLUSIONS

New dehydrodipeptide hydrogelators were prepared using expedite synthetic protocols. Peptide concentration, kinetics of pH dropping (GdL vs hydrochloric acid), and pH (of the broken gels) were shown to influence the gelation process. The most hydrophobic peptide (Npx-L-Trp-Z-ΔPhe-OH, **7a**) formed gels displaying higher elasticity at lower critical gelation concentrations. Gels of peptide **7a** showed irreversible breakup. Although less elastic, gels of peptides **7b** and **7c** exhibited structural recovery and partial healing of the elastic properties. The CD study suggests that naphthalene $\pi-\pi$ stacking interactions are the driving force for peptide self-assembly. The TEM study revealed that all peptides form dense networks of fibers. Self-assembly of peptide **7a** leads to thicker fibers, presumably leading to gels displaying higher elasticity. A potential antitumor compound was successfully incorporated (noncovalently) in the hydrogel of peptide **7a**. The polarity reporting properties of the incorporated drug and FRET experiments allowed us to conclude that the drug is located near or presumably associated with the peptide fibers.

Potential applications, as drug nanocarriers, can be envisaged for this type of hydrogels, for example, as topical formulations.

ASSOCIATED CONTENT

Supporting Information

The Supporting Information is available free of charge on the ACS Publications website at DOI: 10.1021/acs.biomac.5b01006.

UV−vis and CD spectra of aqueous solutions of GdL and hydrolyzed GdL; ^{1}H NMR spectra of compounds **7a**, **7b**, and **7c**; phase diagrams for dehydrodipeptides **7a**, **7b**, and **7c**; photographs of gels obtained by addition of GdL to alkaline solutions of **7a** and **7b** and addition of diluted hydrochloric acid to **7c**; CD and UV−vis absorption spectra and HT data for dehydrodipeptides **7a**, **7b**, and **7c**; stress−strain response curves for penetration tests on hydrogels of dehydrodipeptides **7a−c** (PDF)

AUTHOR INFORMATION

Corresponding Authors

*E-mail: ecoutinho@fisica.uminho.pt.
*E-mail: jmartins@quimica.uminho.pt.
*E-mail: pmf@quimica.uminho.pt.

Notes

The authors declare no competing financial interest.

ACKNOWLEDGMENTS

FCT-Portugal and FEDER/COMPETE through CQ-UM, National NMR Network (Bruker 400), and I3N Strategic Project LA 25:2011-2012. Additional funds by Programa Operacional Regional do Norte (ON.2) through the project Matepro—Optimizing Materials and Processes, with reference NORTE-07-0124-FEDER-000037 FEDER COMPETE are also acknowledged. H.V. also thanks FCT for the PhD grant (SFRH/BD/72651/2010) cofunded by the European Social Fund.

REFERENCES

(1) (a) Li, X.; Du, X.; Li, J.; Gao, Y.; Pan, Y.; Shi, J.; Zhou, N.; Xu, B. *Langmuir* **2012**, *28* (37), 13512−13517. (b) Sutton, S.; Campbell, N. L.; Cooper, A. I.; Kirkland, M.; Frith, W. J.; Adams, D. J. *Langmuir* **2009**, *25* (17), 10285−10291. (c) Nanda, J.; Biswas, A.; Banerjee, A. *Soft Matter* **2013**, *9* (16), 4198−4208.

(2) Yang, Z.; Gu, H.; Zhang, Y.; Wang, L.; Xu, B. *Chem. Commun.* **2004**, *2*, 208−209.

(3) Panda, J. J.; Mishra, A.; Basu, A.; Chauhan, V. S. *Biomacromolecules* **2008**, *9* (8), 2244−2250.

(4) (a) Yang, Z.; Liang, G.; Guo, Z.; Guo, Z.; Xu, B. *Angew. Chem., Int. Ed.* **2007**, *46* (43), 8216−8219. (b) Yang, Z.; Gu, H.; Fu, D.; Gao, P.; Lam, J. K.; Xu, B. *Adv. Mater.* **2004**, *16* (16), 1440−1444. (c) Gao, J.; Wang, H.; Wang, L.; Wang, J.; Kong, D.; Yang, Z. *J. Am. Chem. Soc.* **2009**, *131* (32), 11286−11287.

DOI: 10.1021/acs.biomac.5b01006
Biomacromolecules 2015, 16, 3562−3573

(5) Shi, J.; Gao, Y.; Zhang, Y.; Pan, Y.; Xu, B. *Langmuir* **2011**, *27* (23), 14425−14431.
(6) Chen, L.; Pont, G.; Morris, K.; Lotze, G.; Squires, A.; Serpell, L. C.; Adams, D. J. *Chem. Commun.* **2011**, *47* (44), 12071−12073.
(7) Reddy M, A.; Srivastava, A. *Soft Matter* **2014**, *10* (27), 4863−4868.
(8) Xie, Z.; Zhang, A.; Ye, L.; Feng, Z.-g. *Soft Matter* **2009**, *5* (7), 1474−1482.
(9) Du, X.; Zhou, J.; Xu, B. *Chem. - Asian J.* **2014**, *9* (6), 1446−1472.
(10) Lin, Y.-C.; Hsu, S.-M.; Chang, J.-W.; Liu, Y.-H.; ; Lin, H.-C. *Int. J. Chem. Eng. Appl.* **2015**, *6* (2), 81−85.
(11) (a) Zhao, F.; Ma, M. L.; Xu, B. *Chem. Soc. Rev.* **2009**, *38* (4), 883−891. (b) Gao, Y.; Kuang, Y.; Guo, Z.-F.; Guo, Z.; Krauss, I. J.; Xu, B. *J. Am. Chem. Soc.* **2009**, *131* (38), 13576−13577. (c) Li, J.; Kuang, Y.; Shi, J.; Gao, Y.; Zhou, J.; Xu, B. *Beilstein J. Org. Chem.* **2013**, *9*, 908−917.
(12) Zhang, Y.; Gu, H.; Yang, Z.; Xu, B. *J. Am. Chem. Soc.* **2003**, *125* (45), 13680−13681.
(13) Raeburn, J.; McDonald, T. O.; Adams, D. J. *Chem. Commun.* **2012**, *48* (75), 9355−9357.
(14) Jayawarna, V.; Richardson, S. M.; Hirst, A. R.; Hodson, N. W.; Saiani, A.; Gough, J. E.; Ulijn, R. V. *Acta Biomater.* **2009**, *5* (3), 934−943.
(15) Jayawarna, V.; Ali, M.; Jowitt, T. A.; Miller, A. F.; Saiani, A.; Gough, J. E.; Ulijn, R. V. *Adv. Mater.* **2006**, *18* (5), 611−614.
(16) Huang, Y.; Qiu, Z.; Xu, Y.; Shi, J.; Lin, H.; Zhang, Y. *Org. Biomol. Chem.* **2011**, *9* (7), 2149−2155.
(17) Marchesan, S.; Easton, C. D.; Styan, K. E.; Waddington, L. J.; Kushkaki, F.; Goodall, L.; McLean, K. M.; Forsythe, J. S.; Hartley, P. G. *Nanoscale* **2014**, *6* (10), 5172−5180.
(18) (a) Yang, Z.; Liang, G.; Xu, B. *Chem. Commun.* **2006**, *7*, 738−740. (b) Yang, Z.; Liang, G.; Ma, M.; Gao, Y.; Xu, B. *Small* **2007**, *3* (4), 558−562. (c) Majumder, J.; Das, M. R.; Deb, J.; Jana, S. S.; Dastidar, P. *Langmuir* **2013**, *29* (32), 10254−10263.
(19) Gupta, M.; Bagaria, A.; Mishra, A.; Mathur, P.; Basu, A.; Ramakumar, S.; Chauhan, V. S. *Adv. Mater.* **2007**, *19* (6), 858−861.
(20) Panda, J. J.; Dua, R.; Mishra, A.; Mittra, B.; Chauhan, V. S. *ACS Appl. Mater. Interfaces* **2010**, *2* (10), 2839−2848.
(21) Gupta, M.; Chauhan, V. S. *Biopolymers* **2011**, *95* (3), 161−173.
(22) Vilaca, H.; Pereira, G.; Castro, T. G.; Hermenegildo, B. F.; Shi, J.; Faria, T. Q.; Micaelo, N.; Brito, R. M. M.; Xu, B.; Castanheira, E. M. S.; Martins, J. A.; Ferreira, P. M. T. *J. Mater. Chem. B* **2015**, *3*, 6355−6367.
(23) Nanda, J.; Biswas, A.; Adhikari, B.; Banerjee, A. *Angew. Chem., Int. Ed.* **2013**, *52* (19), 5041−5045.
(24) Martin, A. D.; Robinson, A. B.; Mason, A. F.; Wojciechowski, J. P.; Thordarson, P. *Chem. Commun.* **2014**, *50* (98), 15541−15544.
(25) Adams, D. J.; Mullen, L. M.; Berta, M.; Chen, L.; Frith, W. J. *Soft Matter* **2010**, *6* (9), 1971−1980.
(26) Hughes, M.; Birchall, L. S.; Zuberi, K.; Aitken, L. A.; Debnath, S.; Javid, N.; Ulijn, R. V. *Soft Matter* **2012**, *8* (45), 11565−11574.
(27) (a) Yang, Z.; Liang, G.; Ma, M.; Gao, Y.; Xu, B. *J. Mater. Chem.* **2007**, *17* (9), 850−854. (b) Chen, L.; Morris, K.; Laybourn, A.; Elias, D.; Hicks, M. R.; Rodger, A.; Serpell, L.; Adams, D. J. *Langmuir* **2010**, *26* (7), 5232−5242. (c) Chen, L.; Revel, S.; Morris, K.; Serpell, L. C.; Adams, D. J. *Langmuir* **2010**, *26* (16), 13466−13471.
(28) Li, J.; Kuang, Y.; Gao, Y.; Du, X.; Shi, J.; Xu, B. *J. Am. Chem. Soc.* **2013**, *135* (2), 542−545.
(29) Li, J.; Li, X.; Kuang, Y.; Gao, Y.; Du, X.; Shi, J.; Xu, B. *Adv. Healthcare Mater.* **2013**, *2* (12), 1586−1590.
(30) Queiroz, M.-J. R. P.; Calhelha, R. C.; Vale-Silva, L. A.; Pinto, E.; São-José Nascimento, M. *Eur. J. Med. Chem.* **2010**, *45* (12), 5732−5738.
(31) Oakenfull, D. G.; Parker, N. S.; Tanner, R. I. *J. Texture Stud.* **1988**, *19*, 407−417.
(32) Valeur, B. In *Molecular Fluorescence−Principles and Applications*; Wiley-VCH: Weinheim, 2002.
(33) Crosby, G. A.; Demas, J. N. *J. Phys. Chem.* **1971**, *75* (8), 991−1024.
(34) Fery-Forgues, S.; Lavabre, D. *J. Chem. Educ.* **1999**, *76* (9), 1260.
(35) Kirby, E. P.; Steiner, R. F. *J. Phys. Chem.* **1970**, *74* (26), 4480−4490.
(36) Greenstein, J. P.; Winitz, M. In *Chemistry of the Amino Acids*; Wiley: New York, 1961; Vol. 2.
(37) Chapman, C. J.; Matsuno, A.; Frost, C. G.; Willis, M. C. *Chem. Commun.* **2007**, *38*, 3903−3905.
(38) (a) Ferreira, P. M. T.; Maia, H. L. S.; Monteiro, L. S. *Tetrahedron Lett.* **1998**, *39* (51), 9575−9578. (b) Ferreira, P. M. T.; Maia, H. L. S.; Monteiro, L. S.; Sacramento, J. *J. Chem. Soc., Perkin Trans. 1* **1999**, No. 24, 3697−3703. (c) Ferreira, P. M. T.; Monteiro, L. S.; Pereira, G.; Ribeiro, L.; Sacramento, J.; Silva, L. *Eur. J. Org. Chem.* **2007**, *2007*, 5934−5949.
(39) Adams, D. J.; Butler, M. F.; Frith, W. J.; Kirkland, M.; Mullen, L.; Sanderson, P. *Soft Matter* **2009**, *5* (9), 1856−1862.
(40) Velazquez, M. M.; Valero, M.; Rodríguez, L. J.; Costa, S. M. B.; Santos, M. A. *J. Photochem. Photobiol., B* **1995**, *29* (1), 23−31.
(41) Nakanishi, K.; Berova, N.; Woody, R. W. In *Circular Dichroism Principles and Applications*; VCH Publishers, Inc.: New York, 1994.
(42) Morris, K. L.; Chen, L.; Rodger, A.; Adams, D. J.; Serpell, L. C. *Soft Matter* **2015**, *11* (6), 1174−1181.
(43) Roy, S.; Javid, N.; Sefcik, J.; Halling, P. J.; Ulijn, R. V. *Langmuir* **2012**, *28* (48), 16664−16670.
(44) Lakowicz, J. R. In *Principles of Fluorescence Spectroscopy*, 3rd ed.; Springer: New York, 2006.
(45) Fasman, G. D. In *Handbook of Biochemistry and Molecular Biology, Proteins*, 3rd ed.; CRC Press: Boca Raton, FL, 1976; Vol. *I*.
(46) Chen, L.; Revel, S.; Morris, K.; Adams, D. J. *Chem. Commun.* **2010**, *46* (24), 4267−4269.
(47) Costa, C. N. C.; Hortelao, A. C. L.; Ramos, J. M. F.; Oliveira, A. D. S.; Calhelha, R. C.; Queiroz, M. J. R. P.; Coutinho, P. J. G.; Castanheira, E. M. S. *Photochem. Photobiol. Sci.* **2014**, *13* (12), 1730−1740.
(48) Dobrynin, A. V.; Carrillo, J.-M. Y. *Macromolecules* **2011**, *44* (1), 140−146.
(49) Cardoso, A. Z.; Alvarez Alvarez, A. E.; Cattoz, B. N.; Griffiths, P. C.; King, S. M.; Frith, W. J.; Adams, D. J. *Faraday Discuss.* **2013**, *166* (0), 101−116.
(50) Raeburn, J.; Pont, G.; Chen, L.; Cesbron, Y.; Levy, R.; Adams, D. J. *Soft Matter* **2012**, *8* (4), 1168−1174.
(51) (a) Smith, A. M.; Williams, R. J.; Tang, C.; Coppo, P.; Collins, R. F.; Turner, M. L.; Saiani, A.; Ulijn, R. V. *Adv. Mater.* **2008**, *20*, 37−41. (b) Tang, C.; Ulijn, R. V.; Saiani, A. *Langmuir* **2011**, *27*, 14438−14449.

DOI: 10.1021/acs.biomac.5b01006
Biomacromolecules 2015, 16, 3562−3573